Chemistry–A European Journal

Research Article
doi.org/10.1002/chem.202400785

Chemistry Europe
European Chemical Societies Publishing

www.chemeurj.org

Controlling (E/Z)-Stereoselectivity of –NHC=O Chlorination: Mechanism Principles for Wide Scope Applications

Raed M. Maklad,*[a, b, c] Gamal A. I. Moustafa,*[d, e] Hiroshi Aoyama,[f] and Abdullah A. Elgazar[g]

Organic halogen compounds are cornerstones of applied chemical sciences. Halogen substitution is a smart molecular design strategy adopted to influence reactivity, membrane permeability and receptor interaction. Chiral bioreceptors may restrict the stereochemical requirements in the halo-ligand design. Straightforward (but expensive) catalyzed stereospecific halogenation has been reported. Historically, PCl_5 served access to uncatalyzed stereoselective chlorination although the stereochemical outcomes were influenced by steric parameters. Nonetheless, stereochemical investigation of PCl_5 reaction mechanism with carbamoyl (RCONHX) compounds has never been addressed. Herein, we provide the first comprehensive stereochemical mechanistic explanation outlining halogenation of carbamoyl compounds with PCl_5; the key regioselectivity-limiting nitrilimine intermediate (**8-Z.HCl**); how substitution pattern influences regioselectivity; why oxadiazole byproduct (**P1**) is encountered; stereo-electronic factors influencing the hydrazonoyl chloride (**P2**) production; and discovery of two stereoselectivity-limiting parallel mechanisms (stepwise and concerted) of elimination of HCl and $POCl_3$. DFT calculations, synthetic methodology optimization, X-ray evidence and experimental reaction kinetics study evidence all supported the suggested mechanism proposal (Scheme 2). Finally, we provide mechanism-inspired future recommendations for directing the reaction stereoselectivity toward elusive and stereochemically inaccessible (*E*)-*bis*-hydrazonoyl chlorides along with potentially pivotal applications of both (*E/Z*)-stereoisomers especially in medicinal chemistry and protein modification.

Introduction

Recently, the interest in halogen-containing compounds have been rapidly growing and widely spreading across various research disciplines.[1–3] Alongside their chemical reactivity and high electrophilic nature which render them among the cornerstones of organic synthesis, halo compounds are equally important in medicinal chemistry. Halogen substitution remarkably enhances membrane permeability,[4,5] paving the way for drug targeting to the CNS.[6] Generally, halogen substitution maintains or increases the bioactivity of the parent scaffold[7,8] and/or enhances the availability of drug candidates at their sites of action[9,10] leading to an outstanding role on the antitubercular,[11] anticandidal,[12] antileishmanial-antimalarial,[11] antiproliferative[13,14] along with other bioactivities[10,15] Moreover, β-chloroethylureas,[16] δ-chlorolactones,[17] haloenol lactones,[18,19] 3-halopropiolates,[20] γ-haloallylamines[21] and other electrophilic halo-substituted drug candidates[22] have been reported as potent covalently-bound irreversible receptor inhibitors or protein modifiers of beneficial interests.■■Please check heading levels has set correctly.■■

Keeping into consideration the chiral biological environment, the stereochemical structure of halo compounds have remarkably affected their bioactivities.[23,24] Consequently, the design and development of stereoselective[25,26] and stereospecific[27] halogenation methodologies is considered state-of-the-art.

Phosphorous pentachloride was previously reported to afford stereospecific chlorination of chiral alcohols[28,29] as well as stereoselective chlorination of amides[30,31] and hydroximates[32] (Figure 1A), besides being reported in the halogenation of prochiral carbonyl compounds.[33,34] Generally, the inversion of configuration of secondary chiral alcohols (via S_N2 mechanism)[28] has been noteworthy when compared to the

[a] R. M. Maklad
Pharmaceutical Chemistry Department, Faculty of Pharmacy, Kafrelsheikh University, 33516 Kafrelsheikh, Egypt
E-mail: raed.mostafa@pharm.kfs.edu.eg
raed_mostafa2010@yahoo.com

[b] R. M. Maklad
School of Chemistry, The University of Sydney, 2006 Sydney, New South Wales, Australia

[c] R. M. Maklad
School of Mathematical and Physical Sciences, Faculty of Science, University of Technology Sydney, 2007 Ultimo, NSW, Australia

[d] G. A. I. Moustafa
School of Chemistry, University of Southampton, SO17 1BJ Southampton, U.K.
E-mail: g.a.i.moustafa@soton.ac.uk

[e] G. A. I. Moustafa
Medicinal Chemistry Department, Faculty of Pharmacy, Minia University, 61519 Minia, Egypt

[f] H. Aoyama
Graduate School of Pharmaceutical Sciences, Osaka University, 1-6 Yamadaoka, Suita, 565-0871 Osaka, Japan

[g] A. A. Elgazar
Pharmacognosy Department, Faculty of Pharmacy, Kafrelsheikh University, 33516 Kafrelsheikh, Egypt

Supporting information for this article is available on the WWW under https://doi.org/10.1002/chem.202400785

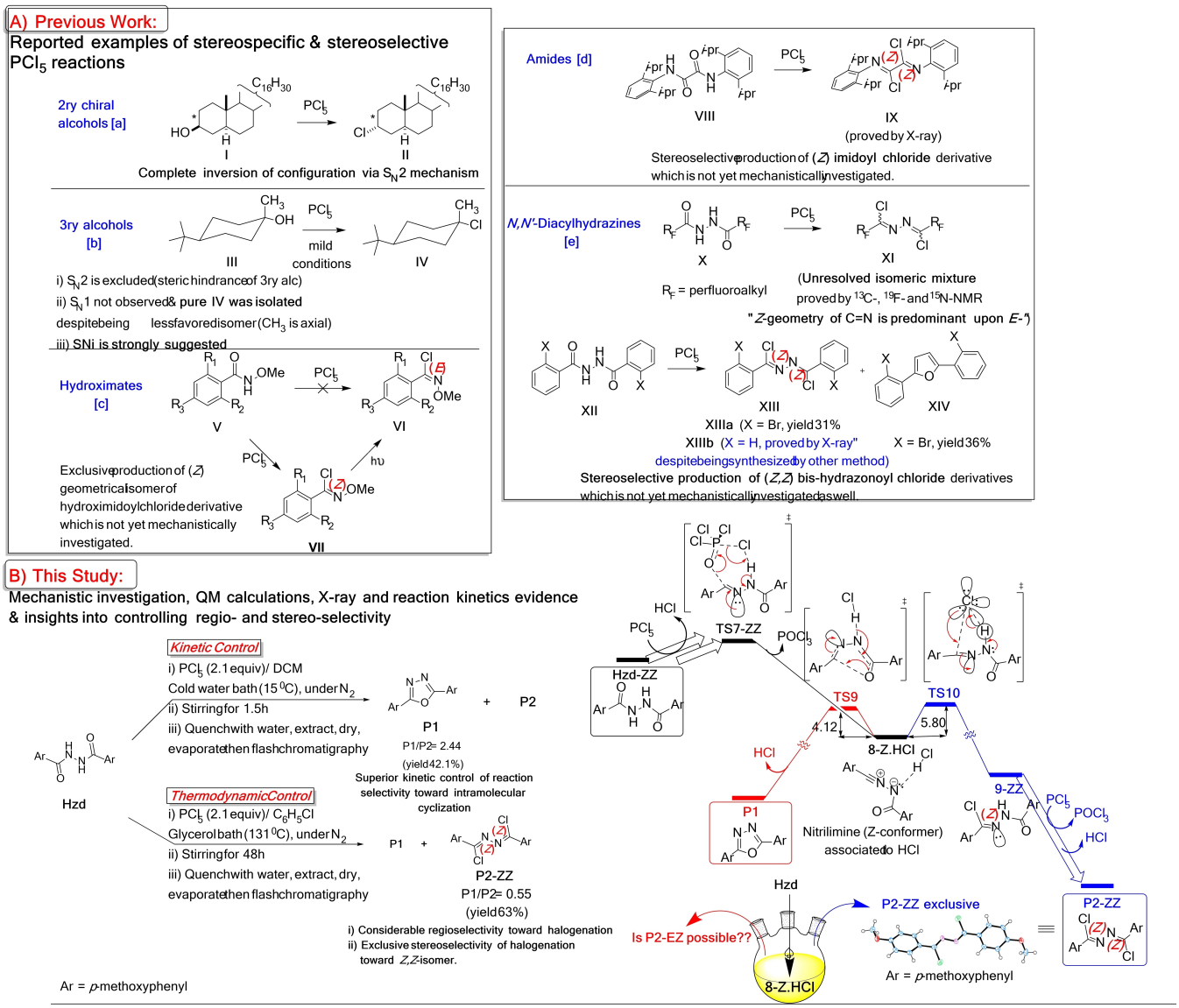

Figure 1. PCl_5-mediated halogenation reactions: A) Previously reported stereoselective and stereospecific chlorination alongside other possible cyclization pathways; B) Current study: *N,N'*-diacylhydrazines as substrates for PCl_5-mediated halogenation, optimized reaction conditions and substituent effect for controlling regio- and stereo-selectivity and DFT-based mechanistic insights supported by X-ray structural evidence of the origin of such selectivity.

analogous less stereospecific $SOCl_2$-mediated chlorination.[28] Despite the predominant configurational retention in sterically-hindered secondary alcohols (due to an alternative S_Ni mechanism),[35] this latter case is nonetheless an exception to the general rule. On the other hand, the PCl_5 reaction with tertiary alcohols usually yields complicated stereochemical outcome unless extremely mild conditions are applied.[29] In this latter case, S_Ni-mediated retention predominates (Figure 1A) over the sterically unfavorable inversion through S_N2 pathway.[29]

Unlike the stereospecific reactions with alcohols, the potential for stereoselective chlorination of carbamoyl compounds (e.g. amides[30,31] and hydroximates[32]) with PCl_5 have hardly been mechanistically studied. In one study,[32] the authors had to utilize a photoisomerization reaction to convert (*Z*)-*O*-methylhydroximidoyl chloride into its (*E*)-isomer instead of direct synthesis of the former from the parent methyl hydroxymate ester and PCl_5 (Figure 1A). Similarly, a stereoselective access to (*Z*)-imidoyl chlorides was gained through reacting the precursor amides with PCl_5,[30,31] the results were undoubtedly confirmed by X-ray crystallography[30,31] (Figure 1A).

Regarding hydrazonoyl chlorides, the predominance of (*Z*)- over (*E*)-isomers has been evidenced by ^{13}C-, ^{19}F- and ^{15}N-NMR study of their unresolved isomeric product mixture upon treatment of perfluoro- *N,N'*-diacylhydrazine precursors with PCl_5[36] (Figure 1A). Despite the previously reported syntheses of X-ray-proved geometrically pure (*Z*)-hydrazonoyl chlorides,[37–41] only two of these studies[41,42] have attributed the stereoselectivity to the chlorination step. Among these two studies,[41,42] only one has utilized PCl_5 as the reagent responsible for the stereoselective chlorination step with no relevant mechanistic study[42] (Figure 1A). Although both studies re-

vealed the X-ray structure of (*Z*,*Z*)-*N*-(chloro(phenyl)methylene)benzenecarbohydrazonoyl chloride (**XIIIb**, Figure 1A),[41,42] the synthetic methodologies were different. The first study[41] utilized Cl_2-mediated chlorination of the corresponding *bis*-hydrazone, while the second one[42] (Figure 1A) included the reaction of PCl_5 with *N*,*N*′-dibenzoylhydrazine.

This latter reaction of *N*,*N*′-diacylhydrazine with PCl_5[43–46] (Figure 1B) has particularly grabbed our attention for the following reasons: A) wide application of the produced *bis*-hydrazonoyl chlorides as reactive building blocks for the synthesis of various heterocycles,[47] directly[48] or *via* a nitrilimine intermediate;[49,50] B) large number of these heterocyclic compounds[51,52] as well as their *bis*-hydrazonoyl chloride precursors[53] are biologically active, some have been reported as irreversible covalent protein modifiers;[54] C) this reaction produces 1,3,4-oxadiazole byproducts[43–46] which are usually bioactive;[55] D) The overall halogenation stereoselectivity has not been attributed to any type of catalysis; E) X-ray structures of the (*E*)-geometrical isomer of hydrazonoyl chlorides at C=N have never been reported before (till the time of writing this article). Moreover, the reaction mechanism outlining the origin of stereoselectivity toward C=N double bond (*Z*)-geometry has not yet been investigated.

Results and Discussion

Experimental Design and Scope of Investigation

The abovementioned facts inspired us with the aim of this study: i) providing the first comprehensive mechanistic investigation outlining the origin of PCl_5-mediated stereoselective halogenation of carbamoyl group; ii) offering mechanism-inspired synthetic recommendations for directing the reaction stereoselectivity toward elusive (*E*)-carbamoyl chloride isomers; and iii) highlighting the synthetic utility, scope, and multidisciplinary applications of the accessed tunable stereoselectivity.

Historically, the PCl_5 reaction with diacylhydrazine derivatives was carried out in different solvents and at variable temperatures.[43–46] The isolated product mixtures usually included the 1,3,4-oxadiazole product and a single isomer (although *E*/*Z* geometries may not be assessed) of *bis*-hydrazonoyl chloride. Sometimes, the authors report the crude reaction yields as exclusively *bis*-hydrazonoyl chloride without elaborate spectral analysis for exclusion of oxadiazole content which confers uncertainty on the claimed hydrazonoyl chloride yields,[56] and motivates toward further investigations.

Firstly, the substituent electronic effects were studied during **Hzd** reaction with PCl_5 (Table S5. Suppl. Mat). Owing to the wide applications of methoxy substitution especially in medicinal chemistry,[57,58] besides its potential stabilization of any expected nitrilium ion intermediates by (+M effect), a representative derivative (**Hzd**$_{(4\text{-OMe})}$ or simply **Hzd**, Figure 1, Scheme 2 and Schemes S1, S2, Table S5 [Suppl. Mat.]) was selected as starting material for extensive study. The effects of reaction temperature, solvent, **Hzd**/PCl_5 molar ratio and the total reaction time on the regioselectivity (**P1**/**P2** ratio) and stereoselectivity (E/Z relative distribution of **P2** isomers) were as well (Tables S1–S5, Suppl. Mat.).

Then, the DFT calculations were utilized to reveal the potential of existence of expected intermediates, assess their reactivities and finally grasp the key selectivity-limiting step(s) in the overall mechanism. After that, a study of reaction kinetics was carried out to validate the mechanism calculations.

Chemical Synthesis of *N*,*N*′-diacylhydrazines Substrates

The starting series of symmetrical *N*,*N*′-diacylhydrazines (**Hzd**) were synthesized from their corresponding carboxylic acids (**Ia–e**) as shown in Scheme 1. Upon neat gentle reflux with four equivalents of thionyl chloride, the carboxylic acids (**Ia–e**) were converted to their corresponding acyl chlorides. Then, the unreacted reagent was distilled off and the produced acyl chlorides were rapidly subjected to hydrazinolysis with half equivalent of 100% hydrazine hydrate (Scheme 1).

Then, two equivalents of the acyl chloride (**II**) were allowed to undergo nucleophilic acyl substitution reaction with one of hydrazine hydrate in the presence of two of triethylamine as base (Scheme 1). As the possibility of *bis*-acylation at the same nitrogen is ruled out due to the relatively higher nucleophilicity of the 1^{ry} NH_2 compared to 2^{ry} carbamoyl NH (the latter being deactivated by resonance), the desired *N*,*N*′-diacylhydrazines (**Hzd**) were obtained in high purity and confirmed by matching their melting points with the reported ones (See the Experimental section for further details). Interestingly, the possibility of mono-acylation could be safely excluded when the acyl chlorides are utilized as start materials,[59] while the same assumption is not valid with the esters[7,13] due to higher reactivity of the former. After that, the resulting *N*,*N*′-diacylhydrazines (**Hzd**) were utilized for the next step after recrystallization from DMF to ensure that the same method was utilized for obtaining pure form of the start materials (**Hzd**) needed for the PCl_5 reaction selectivity study in the next steps.

Optimization Study of Hzd/PCl_5 Reaction Conditions

Concerning the reaction of *N*,*N*′-diacylhydrazine scaffold (**Hzd**) with PCl_5, which is the target topic of this work, several parameters likely to affect the regioselectivity (**P1**/**P2** ratio) alongside the stereoselectivity (*Z*,*Z*-/*Z*,*E*-/*E*,*E*- isomeric ratios of **P2**) were considered during the experimental design. The effect of electronic factors of substitutions, the Hzd/PCl_5 molar ratio, the solvent polarity, the reaction temperature, the overall reaction time (kinetics) were all studied via rationally designed experiments discussed in the Suppl. Mat. in more details (Section 1 and Section 4 [Tables S2–S6]).

Generally, electron withdrawing groups (EWGs) at *para*-position, low **Hzd**/PCl_5 molar ratio favor the **P1** (oxadiazole) formation, while high-boiling-point non-polar solvents, high reaction temperature and increased reaction time promote **P2**

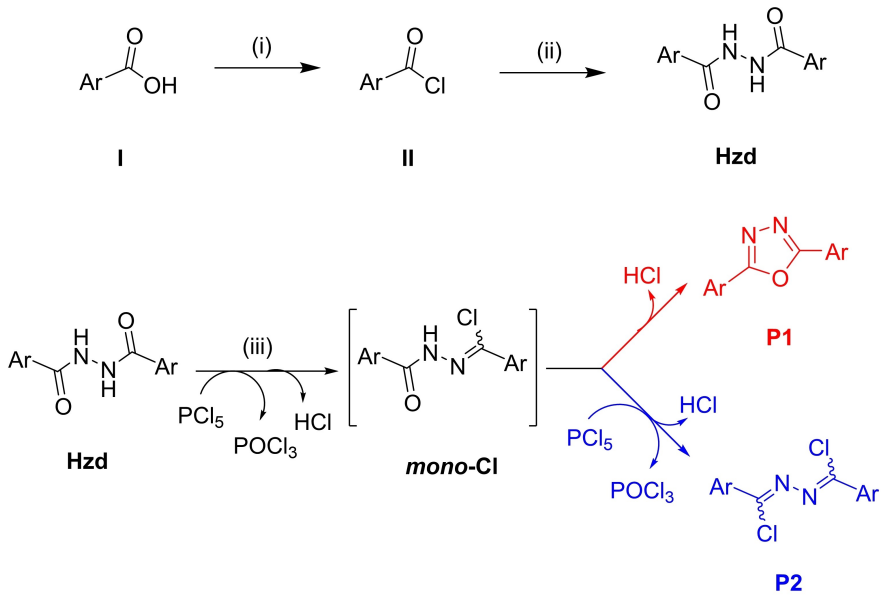

					Ar =
Ia	**IIa**	**Hzd$_{(4\text{-}OMe)}$**	**P1a**	**P2a**	*p*-MeO-C_6H_4
Ib	**IIb**	**Hzd$_{(4\text{-}Me)}$**	**P1b**	**P2b**	*p*-Me-C_6H_4
Ic	**IIc**	**Hzd$_{(4\text{-}H)}$**	**P1c**	**P2c**	C_6H_5
Id	**IId**	**Hzd$_{(4\text{-}Cl)}$**	**P1d**	**P2d**	*p*-Cl-C_6H_4
Ie	**IIe**	**Hzd$_{(4\text{-}NO2)}$**	**P1e**	**P2e**	*p*-NO_2-C_6H_4

Scheme 1. *Reagents and conditions:* (i) $SOCl_2$ (4 equiv.), neat reflux 3 h; (ii) Hydrazine hydrate 100 % (0.55 equiv.)/TEA (2.1 equiv.), DMF, stirring at r.t. overnight; (iii) PCl_5 (0.5–5 equiv)*/Solvent*, N_2 atmosphere, Stirring at −94–40 °C* for 60 sec–72 h*. * See Tables S1–S5 in the Suppl. Mat for detailed reaction optimization methodology.

formation as Z,Z-isomer exclusively (X-ray crystallography section).

Table 1 outlines the optimized reaction conditions needed for a regioselective synthesis of the (Z,Z)- isomer of bis-hydrazonoyl chloride (**P2-ZZ**). The experiment optimization approach depends on preserving the reaction from zero time at thermodynamic control (high temperature) while using the solvent that promotes most the **P2** formation (chlorobenzene, Table S3) and at extended time beyond which no considerable reaction products are expected (48 h, Table S6).

These experimental results strongly suggested that the carbamoyl group halogenation (affording **P2-ZZ**) is the thermodynamic pathway, while the intramolecular cyclization (affording **P1**) is the kinetic one. Yet, deeper mechanistic investigations are still needed to account for such substituent effects, the regioselectivity, unveil the origin of stereoselectivity and offer means of controlling this latter.

Assessment of Stereochemistry of P2-ZZ by Single-Crystal X-Ray Crystallography

Our representative diacylhydrazine **Hzd$_{(4\text{-}OMe)}$** was allowed to react with PCl_5 for 72 h in DCM at 40 °C (Table S5, Suppl. Mat.), reaction quenched, the DCM layer chromatographed and the Hex:EA (9 : 1) fraction was allowed to crystallize for 7 days until the platelet crystals of **P2-ZZ** was obtained (detailed X-ray processing, instrumentation and refinement are included in the Suppl. Mat.). The results undoubtedly confirmed the (Z,Z)-geometries of both C=N groups in **P2-ZZ** (Figure 2) and were deposited with the Cambridge Crystallographic Data Center (CCDC 2102606).

Regardless of the reaction conditions, there was only one exclusive **P2** stereoisomer obtained (as confirmed by matching the ^{1}H NMR spectra in each time with **P2-ZZ** 1H NMR chart displayed in the Suppl. Mat.). This result confirms the sole previous study showing the X-ray structure of Z,Z-isomer of **P2$_{(2\text{-}Br)}$** as the exclusive stereoisomer in similar PCl_5-mediated chlorination (yield 31 %, Figure 1A).[42]

DFT-Based Mechanistic Investigations

The Most Likely Reaction Pathway for the Least Energetic Conformer (Hzd-ZZ)

Schemes 2a–c outline a collective plausible mechanistic proposal of the most kinetically probable pathways of reaction of **Hzd** (as the most likely *Z,Z*-conformer) with PCl_5. More details and discussion about the other less probable mechanism pathways and how they compete together is found in the Suppl. Mat. Generally, our mechanistic investigation was initially

Table 1. The optimized reaction conditions needed for a regioselective synthesis of **P2-ZZ**.

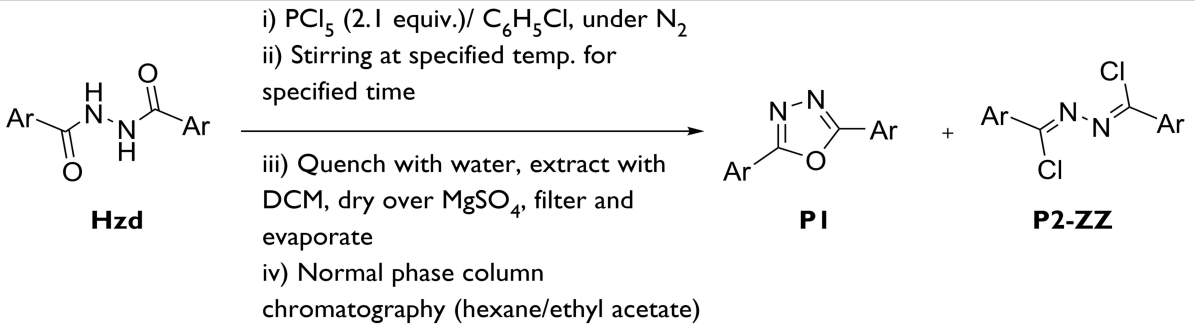

Ar = *p*-MeO-C_6H_4

N,N′-diacylhydrazine derivative	Molar ratio (Hzd: PCl5)	Solvent	Temp (°C)	Rxn Time	[P2-ZZ][a] molar (% yield[c])	[P1][b] molar (%yield[c])	Product ratio (P1/ P2)d	%Hzd recovered[e]
$Hzd_{(4\text{-}OMe)}$	1:2.1	C_6H_5Cl	131	48	0.077238 (63.0%)	0.042542 (34.7%)	0.55	NC

[a] [**P2-ZZ**] was obtained by spectrofluorometry at $\lambda_{ex}=213$ and $\lambda_{em}=526$ nm (Figure S27); [b] [**P1**] was obtained by absorption spectrophotometry at $\lambda=329$ nm (Figure S23); [c] % Yields of **P1** and **P2-ZZ** were calculated by dividing the appropriate product concentration ([**P1**] or [**P2-ZZ**]) by the initial molar concentration of $\mathbf{Hzd}_{(4\text{-}OMe)}$ (in this experiment 0.1226 mol/L); [d] Product ratios were calculated by dividing [**P1**] by [**P2-ZZ**]. [e] NC = not considerable.

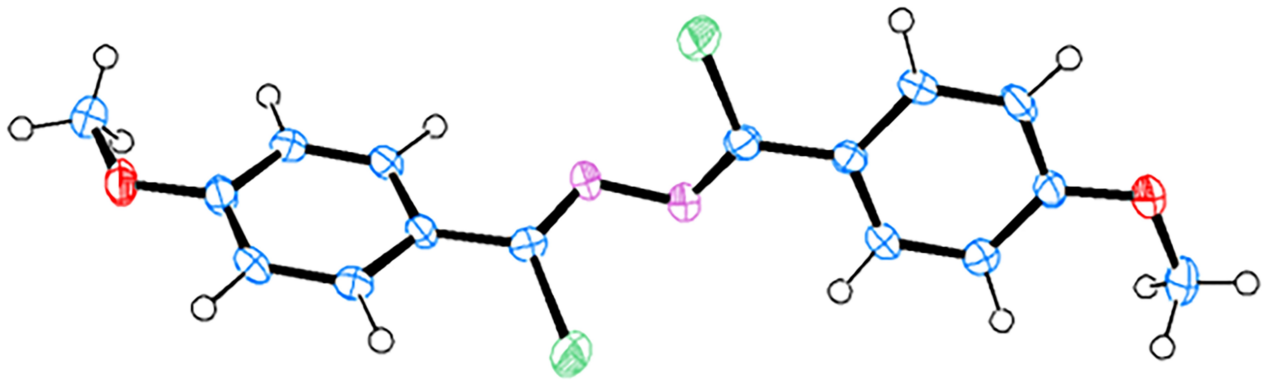

Figure 2. X-ray structure of compound **P2-ZZ** (thermal ellipsoid plot at the 50% probability level).

based upon a firm grasp of a previously reported stable pentacoordinate phosphoranol ether[60,61] as early intermediate involved in PCl_5 reaction with carbamoyl group (here is **6-ZZ**). The discussion below highlights only the key elementary steps, intermediates and transition states controlling the regio- and stereo-selectivity of the whole reaction.

Highlighting the Key Intermediate Controlling the Regioselectivity Step (P1 vs P2 Formation)

Intermediate **8-Z.HCl** was considered as a key one which controls the overall reaction regioselectivity (**P1** *vs* **P2** production) as revealed by the DFT calculation results as it has two distinct highly competitive low-barrier reaction pathways leading to either the oxadiazole **P1** or the mono-hydrazonoyl chloride **9-ZZ** (**TS9** and **TS10**, Scheme 2). The principle of intimate ion pairing suggested in **8-Z.HCl** intermediate was supported by similar previously proven intermediates involving NH-associated chloride ion in a similar PCl_5-mediated chlorination reaction carried out in non-polar solvent.[33]

More insights into the intrinsic reactivity (in terms of the frontier orbital view) of **8-Z.HCl** are discussed in the Suppl. Mat. (Figure S3). It is noteworthy citing a similar *N*-acylnitrilimine intermediate suggested by Giustiniano *et al* as a short-lived *in-situ*-generated precursor to oxadiazole product.[62] Herein, it was computationally found that the oxadiazole product **P1** formation requires only 4.12 kcal/mol barrier (**TS9**, Scheme 2) which accounts for its observation in early stages of the reaction (low temperature and limited-time controls, Tables S3, S5, Suppl. Mat.).

On the other side leading to the *bis*-hydrazonoyl chloride **P2** production, the H-bond stabilized complex **8-Z.HCl** has the tendency to add the HCl molecule covalently and irreversibly to

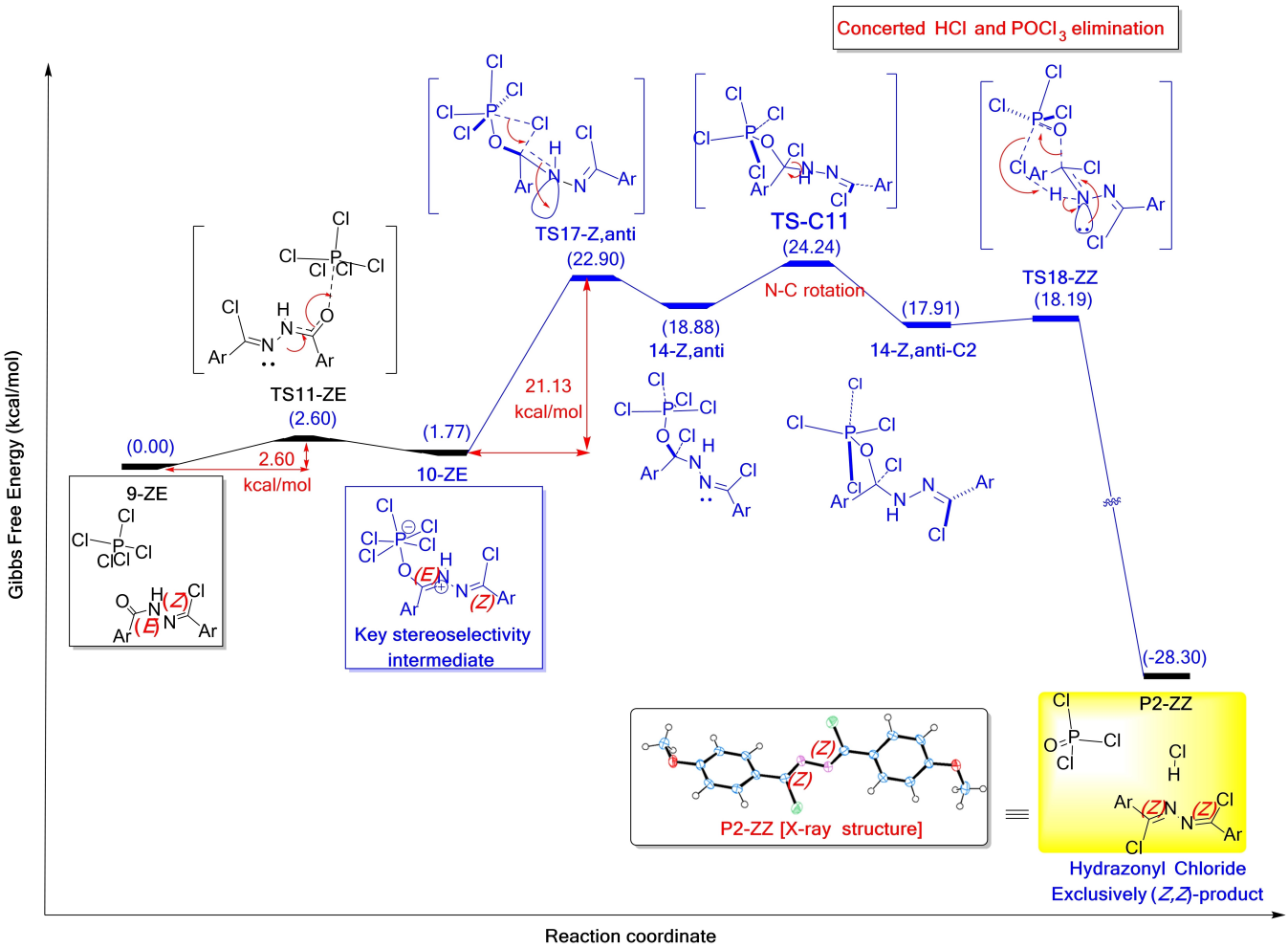

Scheme 2. a Energy profile showing the most kinetically favored mechanism including PCl_5 reaction with **Hzd** (*Z,Z*-conformer) to afford **8-Z.HCl POCl3** as a key intermediate to the final products **P1** (the oxadiazole byproduct) and **P2** (the target halogenation product having multiple stereoisomeric possibilities). Structures labeled with asterisk[*] were optimized at the same 6-31G(d,p) basis set while applying BJ-damping dispersion corrections (B3LYP-D3) and isolated in a separate Potential Energy Surface (PES).

the nitrilimine moiety (via **TS10**) to afford intermediate **9-ZZ** as the first halogenation intermediate leading to **P2** (Scheme 2). This step is computationally expected to involve a low-barrier transition state (**TS10**, 5.80 kcal/mol) which is only 1.68 kcal/mol less than **TS9** (Scheme 2). This justifies why **P2** is less favored at kinetic control conditions (low temperature, Table S4, Suppl. Mat.).

Highlighting the Key Intermediates/Elementary Steps Controlling the Stereoselectivity of the First Halogenation

Intriguingly, it was noticed that the pathway of **8-Z.HCl** through **TS10** (Scheme 2) exclusively produces the (*Z*)-isomer of *mono*-hydrazonoyl chloride **9-ZZ**. This step is considered the first step in the overall halogenation mechanism which controls **P2** product stereochemistry. Although the nitrilimine (**8-Z.HCl**) is linear (no geometrical isomerism), for a nucleophilic addition to the C–N triple bond to occur, the nucleophile (chloride ion) must assume an antiperiplanar geometry to the emerging nitrogen lone pair in the newly emerging sp2 orbital in **TS10** (Scheme 2). In other words, the stereo-electronic factors mentioned earlier[32] generally apply to the addition reactions[62,63] as well as elimination.[32,64] Moreover, the concerted nature of **TS10** is best describing the occurrence of halogenation reaction in non-polar solvents (no ion solvation needed).

The Second Halogenation Step (Discovery of the Addition-Elimination Pathway)

A second attack of PCl_5 molecule proceeds similarly as the first one described earlier (Figure S5, Suppl. Mat.). However, unlike the analogous **TS5** (Scheme 2), **TS12-ZZ** displayed remarkable angle strain and a 31.94 kcal/mol barrier (Figure S5 and relevant discussion, Suppl. Mat.). Alternatively, while applying the Berny algorithm,[65] the possibility of chloride ion intramolecular nucleophilic addition to the C=NH of **10-ZZ** (**TS17-Z,syn**) along with spontaneous and simultaneous $POCl_3$ and HCl elimination

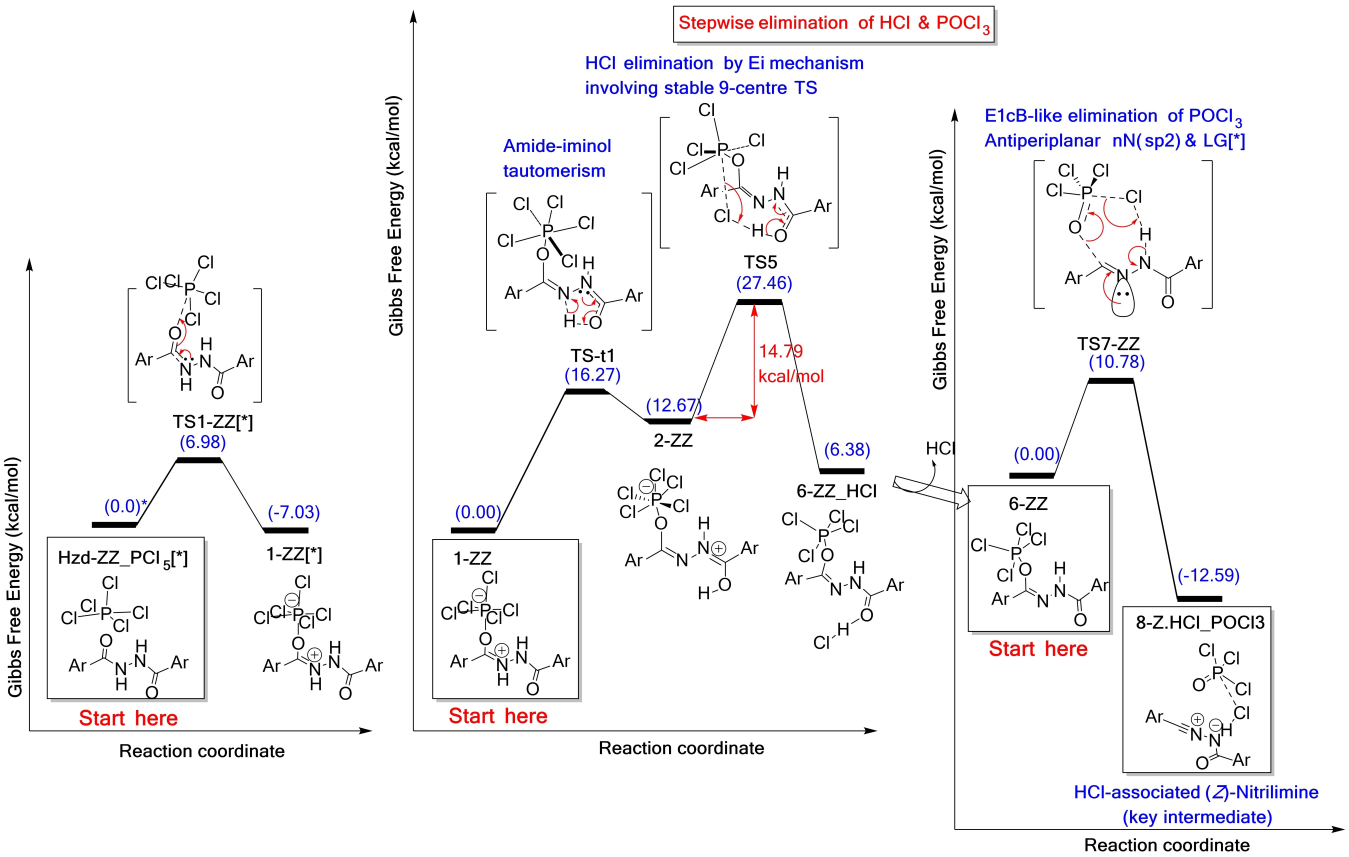

Scheme 2b A] Energy profile showing the regioselectivity-limiting intermediate complex **8-Z.HCl** and the competitive parallel reaction pathways to the oxadiazole byproduct **P1** and the halogenation stereoselectivity-limiting intermediate **9** leading eventually to the target halogenation product stereoisomers (**P2-ZZ** and **P2-EZ**). B] Two energy profiles showing the consecutive reaction pathway of intermediate **9-ZZ** with a second equivalent of PCl5 to provide **P2-EZ** halogenation product (not experimentally isolated). Structures labeled with asterisk[*] were optimized at the same 6-31G(d,p) basis set while applying BJ-damping dispersion corrections (B3LYP-D3) and isolated in a separate PES.

(via Ei mechanism,[66] **TS-18-ZE**) have been discovered (Scheme 2, Figure S14 and relevant discussion [Suppl. Mat.]).

Analogously to **TS17-Z,syn** (leading to **P2-EZ**), **TS17-Z,anti** is also possible, alternative which would account for the experimentally obtained product **P2-ZZ** (Scheme 2 and more detailed discussion in the Suppl. Mat.). Considering both the individual steps involving **TS17-Z,syn** and **TS17-Z,anti** as the rate-limiting ones in their relevant pathways, the question still arises: Why **TS17-Z,anti** pathway is more favored theoretically?? ■■ please mention Scheme 3 before Scheme 4 ■■

Highlighting the Key Intermediates/TSs Controlling the Stereoselectivity of the Second Halogenation Step and the Overall Halogenation Reaction

To answer this abovementioned question, it is worth observing that intermediate **10-ZE** as more thermodynamically stable than its analogue **10-ZZ** (possibly due to additional intramolecular Cl…H association 2.26 and 2.88 °A, Figure 3). Although **TS17-Z,syn** alone has an energy barrier of 22.68 kcal/mol which is acceptable, **TS17-Z,anti** has a lower energy barrier (21.13 kcal/mol) as shown in Figure 3 and Scheme 2. This difference in the activation free energies $\Delta\Delta G^{\ddagger}_{[P2-ZZ/P2-EZ]}$ (1.55 kcal/mol upon applying 6–31G(d,p) basis set and 4.52 kcal/mol upon increasing the calculation accuracy to 6–311 + G(d,p)) justifies the experimental failure to isolate **P2-EZ** along with the exclusive stereoselectivity toward **P2-ZZ** (carbamoyl group Z-halogenation).

To conclude, intermediates **10-ZE** and **10-ZZ** as well as transition states **TS17-Z,anti** and **TS17-Z,syn** are the key ones, and their relative stability is crucial for controlling the overall halogenation stereoselectivity. Controlling the aryl substitution pattern theoretically influences the **10-ZE/10-ZZ and the TS17-Z,anti/TS17-Z,syn** relative stabilities and should subsequently direct the overall halogenation stereoselectivity toward the desired **P2** stereoisomer (discussed later under Scheme 4 and Figures 6, 7).

On the other hand, the addition-elimination mechanism is only applicable to the second halogenation (**TS17** and **TS18**) as the first halogenation usually involves stepwise HCl and $POCl_3$ elimination (**TS5**, **TS7-ZZ**) before chloride addition to the C=N (**TS10**) as shown in Scheme 2 (more discussion in Suppl. Mat.).

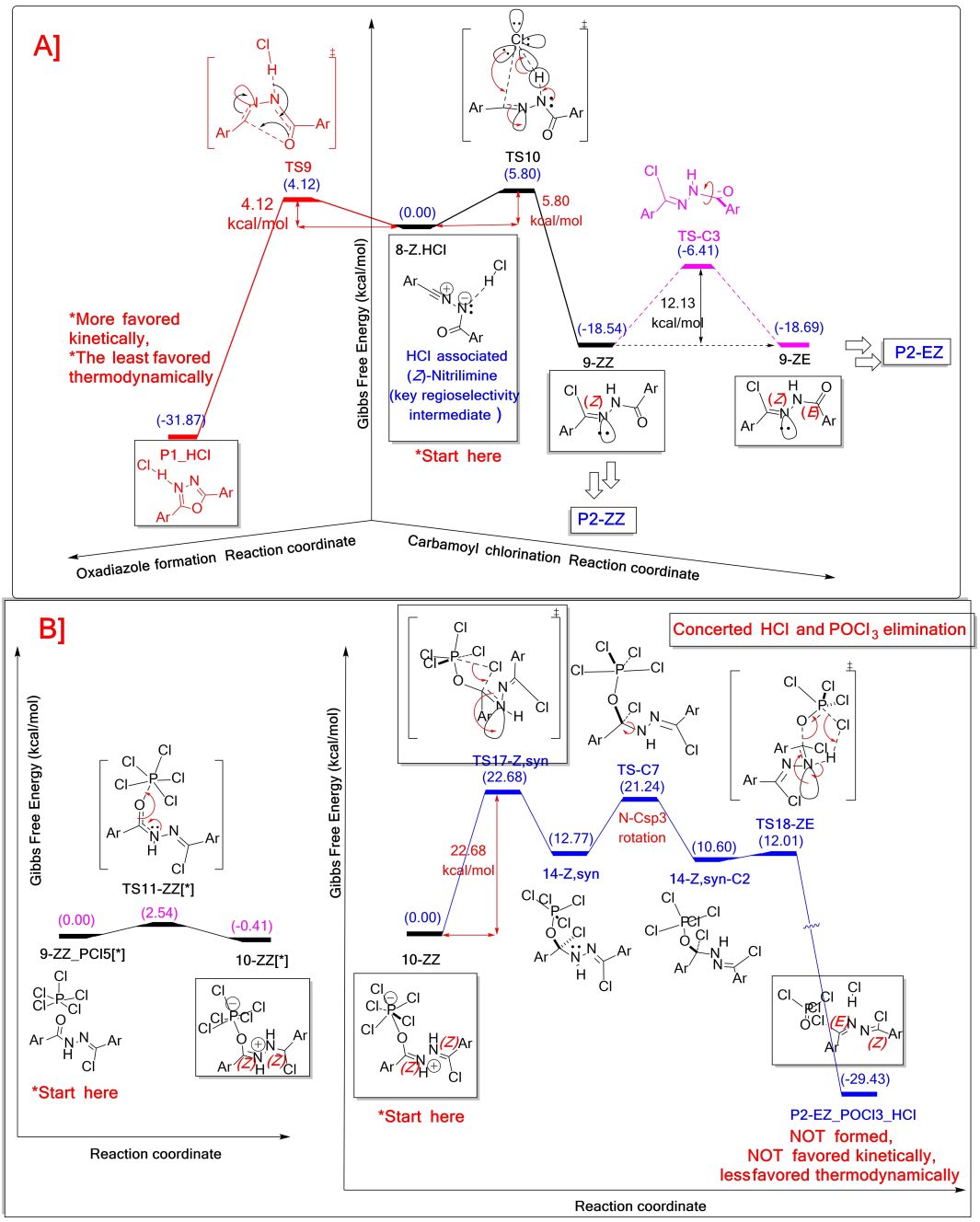

Scheme 2c Energy profile showing the most stereochemically accessible halogenation reaction pathway. Intermediate **9-ZZ** reacts with a second equivalent of PCl5 to provide **P2-ZZ** halogenation product (experimentally identified as the exclusive halogenation product stereoisomer).

How Could N,N′*-diacylhydrazine Conformations Affect the Stereoselectivity of their Reaction with* PCl_5*?*

To this point, we have identified the most prevalent conformer of the diacylhydrazine reactant (**Hzd-ZZ**) and its possible reaction pathways with PCl_5. However, other diacylhydrazine conformers (**Hzd-EZ** and **Hzd-EE**) could also exist and may lead to different stereoselectivity of halogenation and/or afford modified potential to oxadiazole cyclization.

However, there has been agreement that the *Z*-conformer of the N–CO bond is the most stable and prevalent one as long as the N-atom is unsubstituted (as the case presented herein) due to intramolecular H-bonding of the type CO…HN (**Hzd-ZZ**, Scheme 2).[67–72] Price and coworkers[67] experimentally calculated the activation energy of N–CO rotation (by NMR at wide temperature range) to be as low as 20.1 kcal/mol[67] which is comparable to the analogous calculated rotational barriers of **TS-C1** and **TS-C4** reported in this study (Figure 4B). This allowed

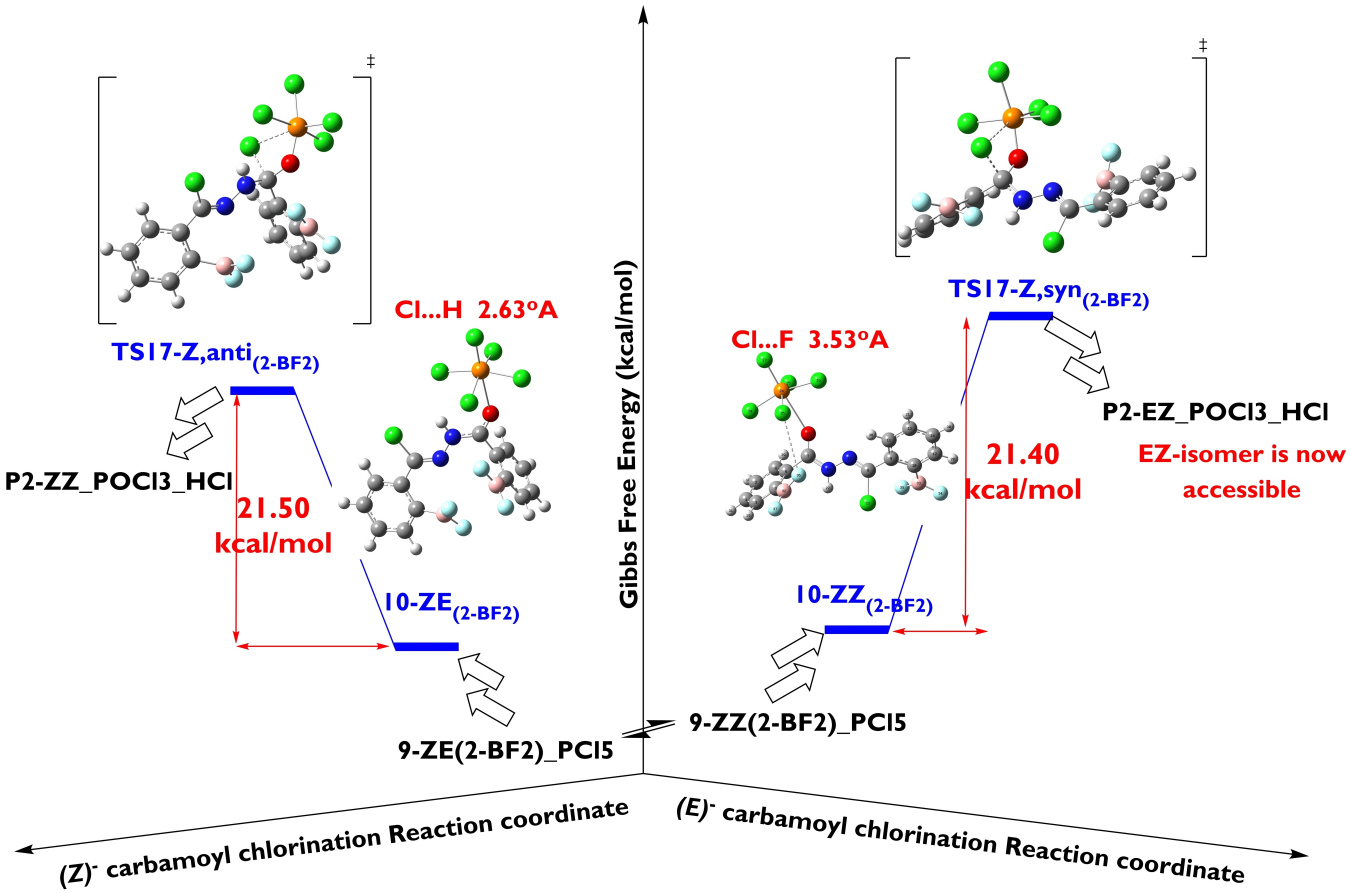

Scheme 3. DFT-based mechanistic evidence that the *ortho*-BF_2 substituent could provide access to controlling the overall halogenation stereoselectivity in favor of the elusive **P2-EZ** stereoisomer. This is shown by the relatively increased stability of the Zwitter-ionic complex **10-ZZ** due to halogen bonding of the PCl_5 chlorine with the *ortho*-BF_2 fluorine. The relative activation energy of **TS17-Z,syn** shows lower barrier relative to **TS-17-Z,anti** in comparison with the data shown before (Figure 3B, leftside). This enhances the possibility of the *E*-halogenation due to the effect of the 2-BF_2 substitution (Ar = 2-BF_2-Phenyl).

free equilibrium between possible rotamers at temperatures above 8 °C.[67]

Nonetheless, the DFT studies of the individual mechanistic pathways of reaction of **Hzd-EZ** and **Hzd-EE** conformers of **Hzd-ZZ** are illustrated in detail in the Suppl. Mat. (Schemes S1, S2 and Figures S6–S16).

Validation of the DFT-Based Mechanistic Investigations

Experimental Results of the C4-Aryl Substitution Effect Study Displayed Absolute Matching with the Theoretical DFT-Based Expectations

Experimentally, as mentioned earlier, the study of the *para*-substituent effects displayed that *para*-NO_2 favors the oxadiazole (**P1**) formation (selectivity factor 1.46 vs 1.33 for the unsubstituted ring), while *para*-OMe (and all electron donating groups) barely influence the reaction regioselectivity (Table S5).

Theoretically, as mentioned earlier, this result evokes a key intermediate (suggested to be **8-Z.HCl**) that is more stabilized by electron-donating groups, thus giving competitive chances of nucleophilic attack either intramolecularly by carbonyl oxygen (**TS9[4-OMe]**, 4.12 kcal/mol barrier) or intermolecularly by chloride (**TS10[4-OMe]**, 5.80 kcal/mol barrier). On the other side, powerful electron withdrawing groups (e.g. *p*-NO_2) strongly destabilize the electrophilic C–N within **8-Z.HCl** molecule and hence do not offer enough time for external nucleophiles such as chloride (**TS10[4-NO_2]**, 9.96 kcal/mol barrier) and alternatively favor intramolecular cyclization affording the oxadiazole **P1** (**TS9[4-NO_2]**, 5.79 kcal/mol barrier) as shown in Figure 5 and Table S7.

Computationally, this theoretical hypothesis (including the expected electronic effect of *para*-substituents) was successfully confirmed by DFT calculations (Figure 5) confirming the same experimentally studied *para*-substituent effects (Table S5, Suppl. Mat.).

Experimental Study of Reaction Kinetics Served Validation of the Theoretical DFT Calculations

To grasp firm evidence on the most plausible reaction mechanism (Scheme 2) and after considering the difficulty separating any isolable reaction intermediate (as mentioned earlier), it was found worthy performing an experimental study

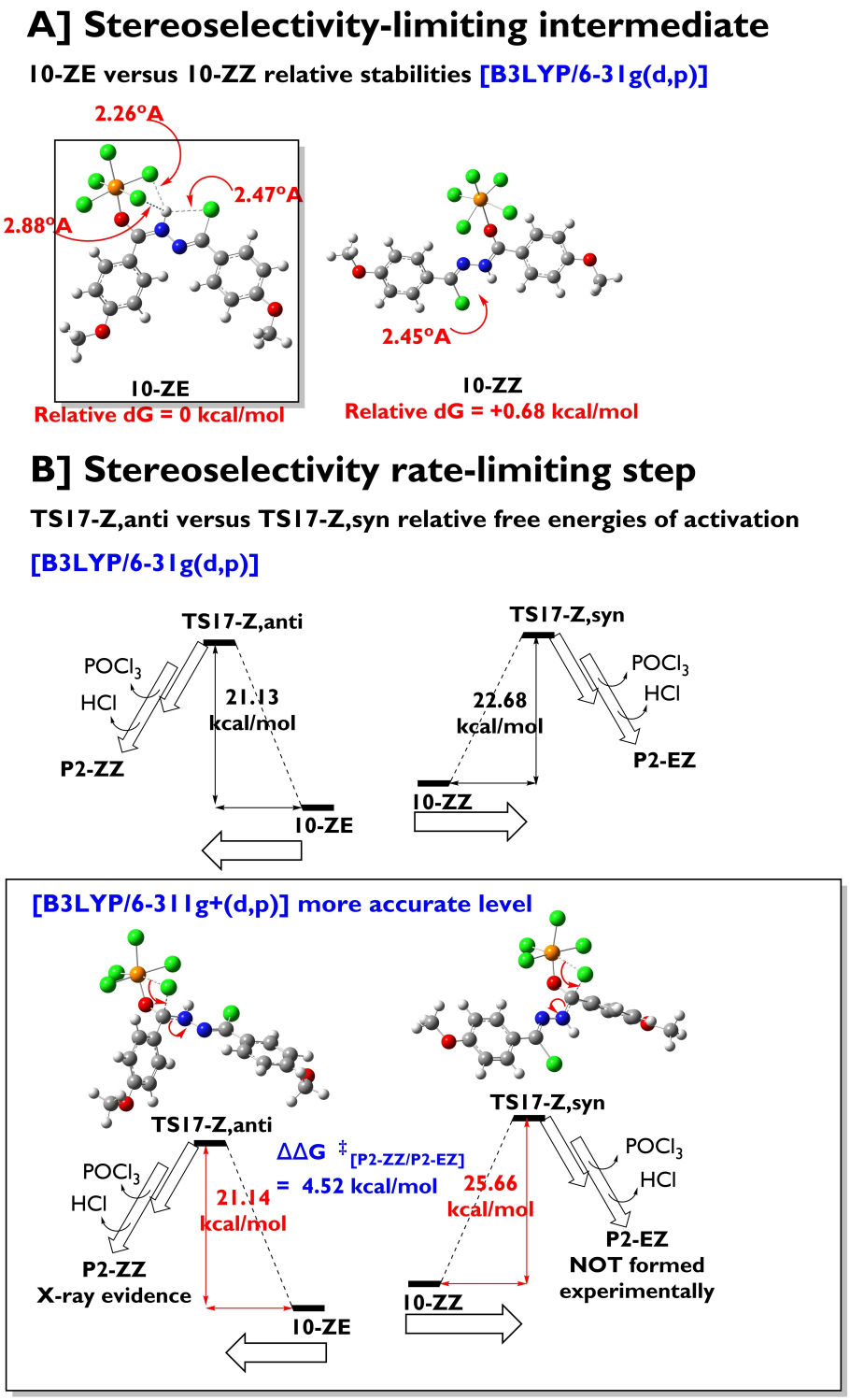

Figure 3. A] Stereoselectivity-limiting intermediate **10** stereoisomers showing superior Cl…H intramolecular association in intermediates **10-ZE** (left side) as compared to **10-ZZ** (right side) explains why the former is more thermodynamically stable and justifies why **10-ZZ** fails to stand out as a discrete energy minimum in the reaction profile (leading to a kinetic disadvantage of **TS17-Z,syn** and **P2-EZ** formation [Scheme 2]). **B]** Stereoselectivity rate-limiting step showing the relative free energies of activation of TS17-Z,anti vs TS17-Z,syn calculated at both the general level B3LYP/6-31G(d,p)] and the more accurate one B3LYP/6-311G + (d,p).

of the kinetics of formation of both reaction products. In principle, this should help us calculate the experimental rate constants at 25 °C and subsequently the difference between the free activation energies of the formation of **P1** and **P2-ZZ** ($\Delta\Delta G^{\ddagger}_{[P1/P2]}$) and compare them with the theoretical calculations. Firstly, the reaction orders with regard to **P1** and **P2-ZZ** production (n1 and n2, respectively) were calculated by the differential method using the following differential rate law

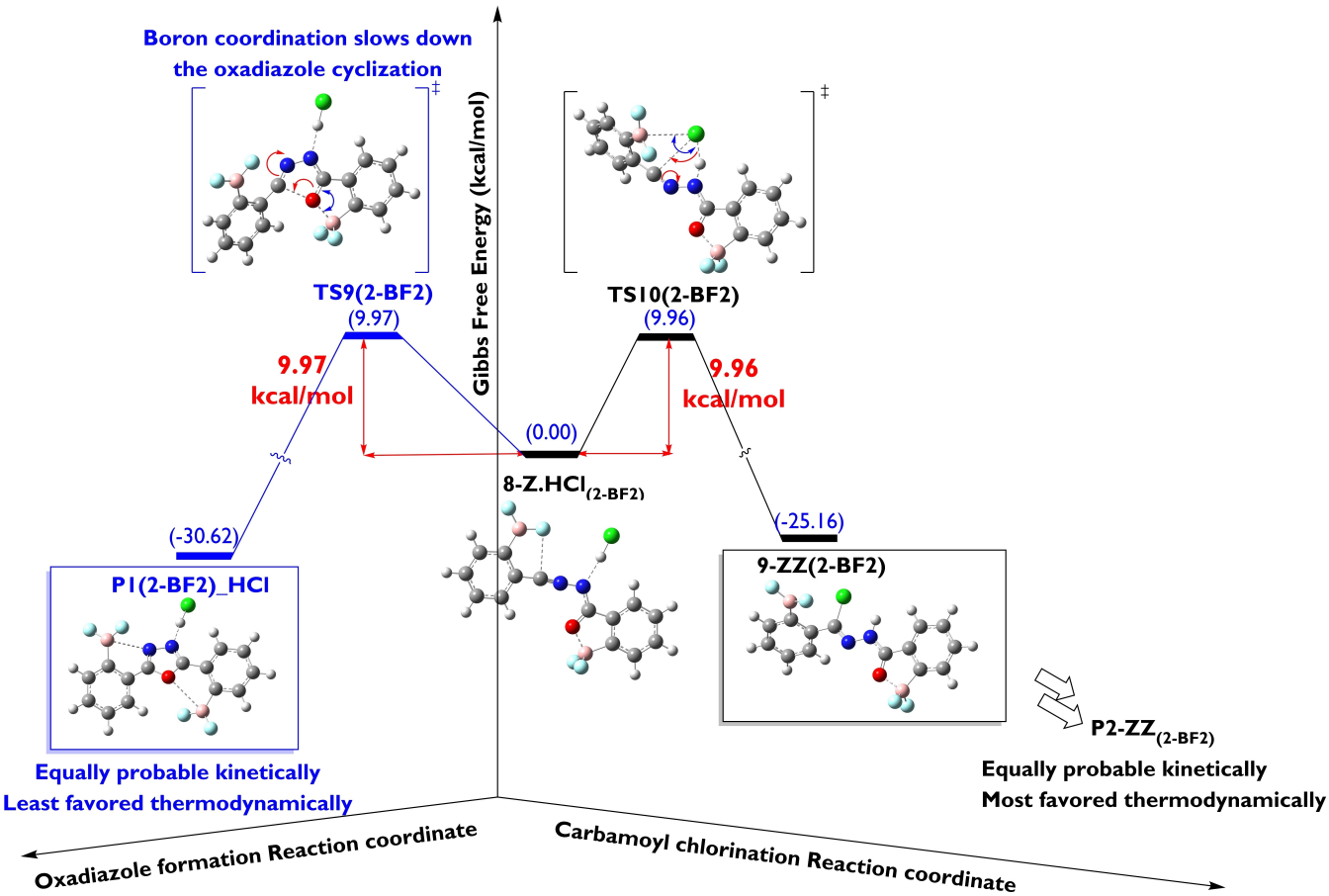

Scheme 4. DFT-based mechanistic evidence that the *ortho*-BF_2 substitution could provide access to controlling the overall reaction regioselectivity to minimize the oxadiazole product (**P1**) and maximize the *bis*-hydrazonoyl chloride (**P2**) as shown by the decreased gab between **TS9** and **TS10** after *ortho*-BF_2 substitution (compare with Scheme 2 where Ar = 4-OMe). The energy profiles in black and blue correspond to the reaction pathways producing the *bis*-hydrazonoyl chloride (**P2**) and the oxadiazole (**P1**) products, respectively.

(assuming approximately constant PCl_5 concentration during the whole reaction time (large excess, Table S6, Suppl. Mat.):■■Equations are not in sequential order hence ordered sequentially. Please check.■■

$$\frac{d[P]}{dt} = k^*[Hzd]^n \tag{1}$$

$$\ln\left[\frac{d[P1]}{dt}\right] = \ln k1 + (n1^*\ln[Hzd]) \tag{2}$$

$$\ln\left[\frac{d[P2-ZZ]}{dt}\right] = \ln k2 + (n2^*\ln[Hzd]) \tag{3}$$

Through monitoring the unreacted hydrazide and the products concentrations by time (Figure S28), the linear rate law Equation (2) provides a straightforward basis for calculation of the reaction orders ($n1$ and $n2$) from the slope and the reaction rate constants ($k1$ and $k2$) from the intercept of the regression equation corresponding to **P1** and **P2-ZZ**, respectively.

Intriguingly, the production of both products followed first order kinetics ($n1 = 1$ and $n2 = 1$), and the rate constants ($k1 = 0.000389\ S^{-1}$ and $k2 = 0.000128\ S^{-1}$) reflect a slightly favored production of **P1** (Figures S29, S30, Suppl. Mat.) which confirms the same reactivity pattern shown by DFT calculations of the selectivity-limiting step (**TS9** and **TS10**, Scheme 2). In principle, where there is competition between products of parallel reactions, the Curtin-Hammett principle[73,74] states that: *"The product distribution reflects the difference in energy between the two rate-limiting transition states"*. Accordingly, by substitution of the experimental $k1$ and $k2$ values in the linear form of Curtin-Hammett law (Equation 4), the experimental $\Delta\Delta G^{\ddagger}_{[P1/P2]}$ will be equal to 0.66 kcal/mol at room temperature (T = 298 °K = 25 °C, Table S6, Suppl. Mat.).

$$\ln\frac{k1}{k2} = -\frac{\Delta\Delta G^{\ddagger}_{[P1/P2]}}{RT} \tag{4}$$

On the other side, according to the DFT calculations of free energies at 298 °K (Tables 2 [entries 3,4] and S7), the theoretical $\Delta\Delta G^{\ddagger}_{[P1/P2]}$ value can be easily calculated as follows:

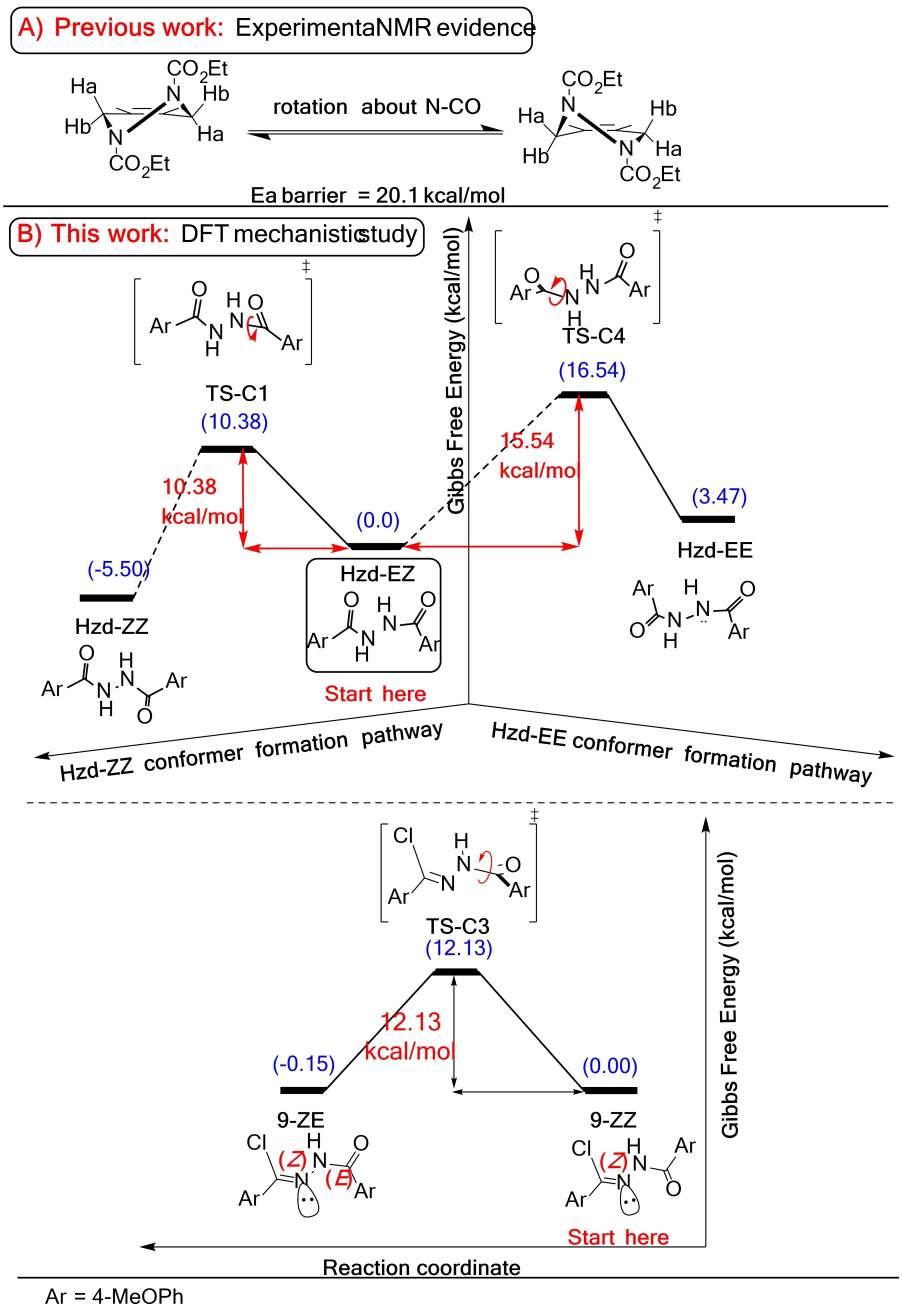

Figure 4. A) Previous work showing NMR experimental calculation of the energy barrier of N–CO conformation of an alicyclic diacylhydrazine derivative which confirms a free equilibrium between possible rotamers at temperatures above 8 °C;[67] **B)** The DFT study carried out in this work confirming the potential of free equilibrium of all **Hzd** N–CO conformers at temperatures lower than room temperature. **Hzd-ZZ** prevails among the other possible conformers of the carbamoyl start material **Hzd** which suggests the predominance of its reaction pathway. Intermediate **9** conformers (**9-ZZ** and **9-ZE**) are expected to be in semi-equimolar equilibrium state leaving the reaction pathways of both with PCl_5 accessible and dependent on the rate-limiting steps of each individual pathway (formation of **TS17-Z,syn** and **TS17-Z,anti**, respectively).

$$-\Delta\Delta G^{\ddagger}_{[P1/P2]} = \Delta G^{\ddagger}_{[P2]} - \Delta G^{\ddagger}_{[P1]}$$

Given that the free energies of activation of **P1** and **P2-ZZ** formation are corresponding to the selectivity checkpoint at **8-Z.HCl** at which two parallel pathways compete with one another via **TS9** and **TS10** to afford **P1** and **P2-ZZ** (Scheme 2), the calculated $\Delta\Delta G^{\ddagger}_{[P1/P2]}$ was found to be 1.68 and 0.61 kcal/mol based on the 6–31G(d,p) and the 6–311+G(d,p) theoretical levels, respectively (Table 2 [entries 3,4]).

In conclusion, a small value of 0.05 kcal/mol deviation of the calculated from the observed difference in reaction barriers of both **P1** and **P2-ZZ** production ($\Delta\Delta G^{\ddagger}_{[P1/P2]}$) stands out as firm evidence of the validity of the suggested reaction mechanism (Scheme 2) and the reliability of the DFT calculation methodology (Suppl. Mat.).

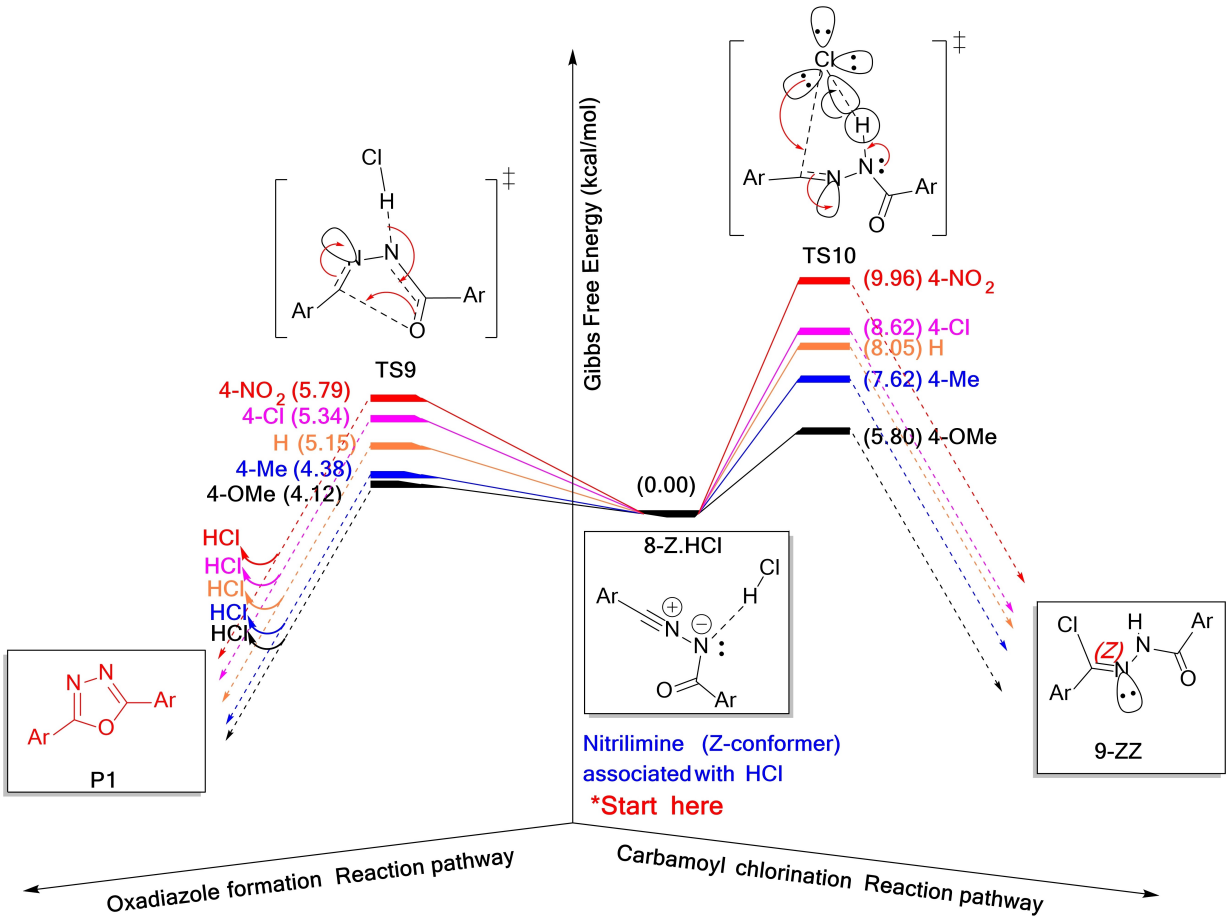

Figure 5. Energy profiles showing the substituent effect on the reactivity of the key intermediate **8-Z.HCl** at the regioselectivity step in the whole reaction (competition of **TS9** leading to **P1** with **TS10** leading eventually to **P2**). Energy profiles corresponding to different substitution patterns are aligned at the **8-Z.HCl** point for easy comparison purposes. The results suggest that the *para*-substitution pattern affects both **TS9** and **TS10** equally likely through electronic effects (electron-donating groups more favored) without altering the relative reactivities towards either pathway (**TS9** and **P1** formation are still slightly more favored under kinetic control). The *p*-nitro group is an exception as it considerably favors **P1** production by 4.17 kcal/mol.

Table 2. Determination of the degree of reliability of the selected theoretical level 6–31G(d,p) for general application in the mechanistic studies in this article. This table shows the deviations (mean error) of the double-ζ 6–31G(d,p) from the more accurate triple-ζ 6–311+G(d,p) results of the calculation of the reaction energetics ($\Delta G^{\ddagger}$ and $\Delta H^{\ddagger}$) of the rate-limiting and selectivity-limiting reaction steps.

Entry	Reaction step	Free energy barrier ($\Delta G^{\ddagger}$ in kcal/mol)			Enthalpy barrier ($\Delta H^{\ddagger}$ in kcal/mol)		
		6-311+G (d,p)	6-31G (d,p)	error	6-311+G (d,p)	6-31G (d,p)	error
1	2-ZZ to TS5	13.50	14.79	+1.29	13.25	14.39	1.14
2	6-ZZ to TS7-ZZ	9.79	10.78	+0.99	10.86	12.09	1.23
3	8-Z.HCl to TS9	5.77	4.12	−1.65	3.35	2.21	−1.14
4	8-Z.HCl to TS10	6.38	5.80	−0.58	3.59	2.99	−0.60
5	10-ZZ to TS17-Z,syn	25.66	22.68	−2.98	19.39	17.15	−2.24
6	10-ZE to TS17-Z,anti	21.14	21.13	−0.01	19.38	19.89	0.51
7	**Mean error**			1.25			1.33

Experimental Results of the Solvent Effect Study Displayed Absolute Matching with the Theoretical DFT-Based CPCM Solvation Results

The previously discussed results of the experimental synthetic optimization of the "Effect of Solvent" (Section 1.1.3. and Table S3, Suppl. Mat.) were utilized as reference for the validation of the employed Conductor-like Polarizable Continuum solvation Model (CPCM) as compared to the gas-phase calculations. The CPCM results (shown in Table S7c) displayed that the same equilibrium predominance of **Hzd-ZZ** conformer would be encountered in each of the six solvents studied

(experimentally and computationally). Additionally, the calculated free energy barriers of the first halogenation step (via TS10) demonstrated decreasing values (against the alternative barriers of formation of the oxadiazole **P1** via TS9) as the solvent polarity decreases (till only 0.06 kcal/mol difference between TS10 and TS9 barriers is reached in chlorobenzene, Table S7c). This confirms the experimental observation that the hydrazonoyl chloride formation is most favored regio-selectively in chlorobenzene as compared to other solvents (Tables S3 and 1).

Furthermore, the rate-limiting step of the *bis*-hydrazonoyl chloride **P2-ZZ** formation (formation TS17-Z,anti) displayed no significant change in the kinetic barrier upon changing the solvent. This gives inspirations that the solvent effect has little to do with the stereoselectivity and other factors are involved (e.g. substituent effect and the *o*-BF2 group discussed later).

Computational Validation by Comparison with Results from High Accuracy Calculation Level

The reliability of the selected level of the DFT theory (6-31G(d,p)) for accurate calculation of the reaction barriers was ensured by re-examining with the split-valence triple-ζ basis set 6–311 + G(d,p) with diffusion function. Then, the reaction barrier energetics ($\Delta G^{\ddagger}$ and $\Delta H^{\ddagger}$) of the rate-limiting and selectivity-limiting steps were re-extrapolated. The results are listed in Table 2 showing the mean error of the currently employed method of calculation of $\Delta G^{\ddagger}$ and $\Delta H^{\ddagger}$ values (in kcal/mol as compared to the high-level method) and revealing that such a low mean error range of 1.25 and 1.33 kcal/mol in the evaluation of $\Delta G^{\ddagger}$ and $\Delta H^{\ddagger}$, respectively, would be expected upon generalizing the calculations at the lower basis set. Additionally, Figure 5 shows how the stereoselectivity limiting formations of TS17-Z,syn and TS17-Z,syn are compared at both calculation levels. These results, coupled with the experimental results of reaction kinetics (and other sources of evidence discussed above) emphasize the validity of the suggested reaction mechanism and the calculation methods employed.

Mechanism-Guided Insights into Directing the Reaction Stereoselectivity Toward the (E,Z)- Stereoisomer of bis-*Hydrazonyl Chloride (P2-EZ).*

After gaining more computational knowledge about the **Hzd** reaction with PCl_5, the key intermediate controlling the C=N stereochemistry in the final **P2** product isomer (namely **9-ZZ**) has been clearly envisioned (Scheme 2). Moreover, the DFT study revealed an inherent driving force of **9-ZZ** to undergo conformational conversion to **9-ZE** until an equilibrium is reached which includes considerable concentrations of both C(O)–N rotamers at room temperature (only 12.13 kcal/mol barrier, Scheme 2).

At this point, **9-ZZ** is likely to exhibit no tendency to proceed to a subsequent reaction with PCl_5 due to relatively higher free energy barrier in the rate-limiting step leading to **P2-EZ** (**TS17-Z,syn** alone has an energy barrier of 22.68 kcal/mol). On the other hand, **TS17-Z,anti** (the rate-limiting TS leading from **9-ZE** to **P2-ZZ**) has a lower energy barrier (21.13 kcal/mol) as shown in Figure 3 and Scheme 2. This difference in the activation free energies $\Delta\Delta G^{\ddagger}_{[P2-ZZ/P2-EZ]}$ (1.55 kcal/mol at 6–31G(d,p) basis set and 4.52 kcal/mol at 6–311 + G(d,p) basis set) justifies the experimental failure to isolate **P2-EZ** along with the exclusive stereoselectivity toward **P2-ZZ** (carbamoyl group Z-halogenation).

These findings justify the exclusive production of the (Z)-carbamoyl compound (e.g. **P2-ZZ** hydrazonoyl chloride herein and in previous study[42]) in terms of the higher stability of the (*E*)-tetrachlorophosphoranolimine precursor to the (*Z*)- final product (e.g. **10-ZE**) along with the relatively lower energy barrier of (*Z*)-halogenation (e.g. via **TS17-Z,anti**) as shown in Figure 3.

Therefore, a rational intervention to provide access to the elusive (*E*)-carbamoyl stereoisomer (e.g. **P2-EZ**) would involve enhancement of the relative stability of the Zwitter-ionic precursor complex (e.g. **10-ZZ** as compared to **10-ZE**, Figure 3). This might be accomplished by introducing a source of intramolecular attraction forces among Cl atoms and an additionally introduced aromatic substituent in **10-ZZ** which should mimic the intramolecular Cl…HN hydrogen bonds in **10-ZE** (Scheme 3). Accordingly, we suggested introducing one *ortho*-BF_2 to the *bis*-hydrazide functionality on each aromatic ring in **Hzd** (to reserve the **Hzd** molecule symmetry, Scheme 3). The *ortho*-substituent was carefully selected so that the electron-rich Cl atom (within the $-OPCl_5$ group) could develop a potential to bind the vacant p-orbital in the electron-poor boron atom *via* a coordination bond. Intriguingly, this approach has displayed success to locate the Zwitter-ionic complex **10-ZZ$_{(2\text{-}BF2)}$** which stands out as a stable intermediate between **TS11-ZZ$_{(2\text{-}BF2)}$** and **TS17-Z,syn$_{(2\text{-}BF2)}$** (Scheme 3). In a manner of speaking, **TS17-Z,syn$_{(2\text{-}BF2)}$** has been deemed not only accessible (21.40 kcal/mol), but also competitive and more kinetically favored than **TS17-Z,anti$_{(2\text{-}BF2)}$**. Of note is that the DFT optimized structure of **10-ZZ$_{(2\text{-}BF2)}$** displayed F…Cl halogen bonding interaction of 3.53 °A which is stronger than its analog in **TS11-ZZ$_{(BF2)}$** (4.84 °A). This halogen bonding interaction may account for the increased stability of **10-ZZ$_{(2\text{-}BF2)}$** as compared to **10-ZZ** more precisely than our preliminary assumption of Cl…B coordination. Interestingly, this (in principle) expands the synthetic scope of possible *ortho*-substituents to all α-fluorinated groups (e.g. CF_3 which is popular in medicinal chemistry).

To conclude, in this work we introduce the aromatic α-fluorinated groups as a clue for the reversal of the stereoselectivity of the overall chlorination reaction toward the elusive (*E,Z*)-stereoisomer of *bis*-hydrazonoyl chloride (**P2-EZ**, Scheme 3) without employing any catalysis.

Mechanism-Guided Insights into Directing the Reaction Regioselectivity Toward the Production of bis*-Hydrazonyl Chloride P2*

Given that the experimental product yields under variable reaction conditions (Tables S2–S6, Suppl. Mat.) provided a straightforward way of enhancing the reaction regioselectivity toward the oxadiazole product (**P1**), we are now theoretically demonstrating the potential of reversing the regioselectivity toward the *bis*-hydrazonoyl chloride (**P2**). Fortunately, we have already outlined experimentally the role of *para*-electron donating groups, solvent, reaction temperature and overall time in the optimized **P2** production conditions discussed above (up to 63% yield of **P2** with a selectivity factor of 1.82 over **P1** under thermodynamic control, Table 1). Moreover, the computational insights offered better understanding by highlighting the key intermediate and the competing transition states controlling the reaction regioselectivity (namely **8-Z.HCl**, **TS9** and **TS10**, respectively) and justified the need for thermodynamic control by the computational fact that **TS10** (leading to **P2**) is 1.68 kcal/mol less favored than **TS9** (leading to **P1**) as shown in Scheme 2.

However, the fact that *para*-substitution has little to do with controlling the relative ratios of **P1** and **P2** (Figure 5) induced our curiosity about tuning the *ortho*-substituents for altering the relative stabilities of **TS9** and **TS10** as compared to intermediate **8-Z.HCl** aiming to confer higher kinetic advantage on **P2**. In principle, if the C=O oxygen in **8-Z.HCl** got involved in a coordination bond (e.g. with an *ortho*-substituent on the nearby aromatic ring), it would be less likely to initiate the intramolecular cyclization of **8-Z.HCl** to the unwanted oxadiazole (**P1**) giving a better chance to the competing pathway leading to intermediate **9-ZZ** and finally to the desired *bis*-hydrazonoyl chloride **P2** (Scheme 4). The need for an electron acceptor *ortho*-substituent has drawn our curiosity to re-employ the BF_2 group, but this time as a regioselectivity enhancer toward favored *bis*-hydrazonoyl chloride (**P2**) production minimum production of the undesirable oxadiazole product (**P1**).

The results shown in Scheme 4 intriguingly confirmed our hypothesis. Generally, the *o*-BF_2 conferred higher relative stability on the key regioselectivity intermediate (**8-Z.HCl**$_{(2BF2)}$) as compared to both **TS9**$_{(2BF2)}$ (leading to **P1**$_{(2BF2)}$ and **TS10**$_{(2BF2)}$ (leading to **P2**$_{(2BF2)}$). The is best explained in terms of boron Lewis acidic coordination of the C=O nucleophilic end along with fluorine Lewis basic stabilization of the nitrilium electrophilic end of **8-Z.HCl**$_{(2BF2)}$ molecule. Regarding the Lewis acidic effect of the *o*-BF_2, both **TS9**$_{(2BF2)}$ and **TS10**$_{(2BF2)}$ were badly influenced by boron coordination of the transition state nucleophilic moieties (C=O oxygen and the chloride ion, respectively) leading to noticeably increased barriers of both transition states (Scheme 4). However, what is unique about **TS10**$_{(2BF2)}$ is that boron coordination of the chloride nucleophilic motif occurs at the expense of slight conformational changes in the ArC–B bond carrying the *o*-BF_2 group leading to loss of the Lewis basic stabilization of the electrophilic nitrilium C–N motif (by fluorine) and rendering it more reactive toward chloride ion (**TS10**$_{(2BF2)}$, Scheme 4).

Overall, the relative computational stabilities of **TS9**$_{(2BF2)}$ and **TS10**$_{(2BF2)}$ have been successfully inverted by the *o*-BF_2 group. After adopting the *o*-BF_2 directing group hypothesis, **TS10**$_{(2BF2)}$ is now 0.01 kcal/mol more kinetically favored than **TS9**$_{(2BF2)}$ (and so is **P2** over **P1**) rather than being 1.68 kcal/mol less favored (which has been encountered in case of **TS10** as compared to **TS9** where no *o*-BF_2 was introduced) as shown in Scheme 4.

Synthetic Inspirations, Recommendations, and Wide Scope Potential Applications

As mentioned above in the Introduction, the capacity to implement stereoselective halogenation could have multidisciplinary scientific applications. After optimizing the experimental conditions for regioselective and stereoselective production of hydrazonoyl chloride (**P2-ZZ**) and then applying the gained mechanistic principle of utilizing the *o*-BF_2 as regioselectivity enhancer (to minimize **P1** byproduct) and stereoselectivity inverter (giving access to **P2-EZ**), we had better now head to the applications. In Figures 6 and 7, we have summarized the most promising applications anticipated for the stereoselective synthesis of the chloroimidoyl (Cl–C=N–) group by applying the synthetic and theoretical principles discussed above.

Several examples of biologically active scaffolds with imine (C=N) linkers have been reported to offer beneficial intervention in cancer,[75–77] inflammatory cancer[77] and antimicrobial[78] therapies. Hydrazones,[75–77] hydrazone-1-carboximidamides,[78] semicarbazones[77] and thiosemicarbazones.[75–77] Some of them have displayed considerable target protein subtype selectivity (e.g. HCA II in cancer chemotherapy[75]) while showing (*E*)-configuration of the C=N as proved by X-ray structural analysis.[75] Our adopted synthetic strategy would provide access to (*Z*)-isomers of those bioactive imine-linker scaffolds (Figure 6A) which should influence their bioactivity or target enzyme subtype selectivity through straightforward (*Z*)-hydrazonoyl chloride intermediates stereoselectively synthesized as described herein.

On the other side, the (*E*)-configuration of the C=N could be analogously beneficial. It has been well-established that tubulin inhibitors of the combretastatin A-4 (CA-4) family have got a unique *cis*-restricted *vic*-diaryl structure in common.[79] In addition, the successful design of a potent CA-4 analog with a conjugated (*E,Z*)-diene linker[80] along with our promising anti-tubulin activity results about (*E*)-hydrazonoyl chlorides (under preparation for publication)[59] have inspired us with the (*E,Z*)-*bis*-hydrazonoyl chlorides in Figure 6B. The *ortho*-Boronic acid should be accessible via hydrolysis of *o*-BF_2 (the stereoselectivity modulating group) and fortunately acting as a bioisostere of the OH in CA-4 with anticipated better solubility for clinical trials.[81,82]

It might be of special interest to utilize the (*E,Z*)-*bis*-hydrazonoyl chloride stereoisomer (accessed through the *o*-BF_2 stereoselectivity modulating group) for the synthesis of functionalized macrocycles (Figure 6c). The cyclization would employ a bifunctional boronic acid stereoselective cross-coupling reaction with the *bis*-hydrazonoyl chloride Cl–C=N sp2-hybri-

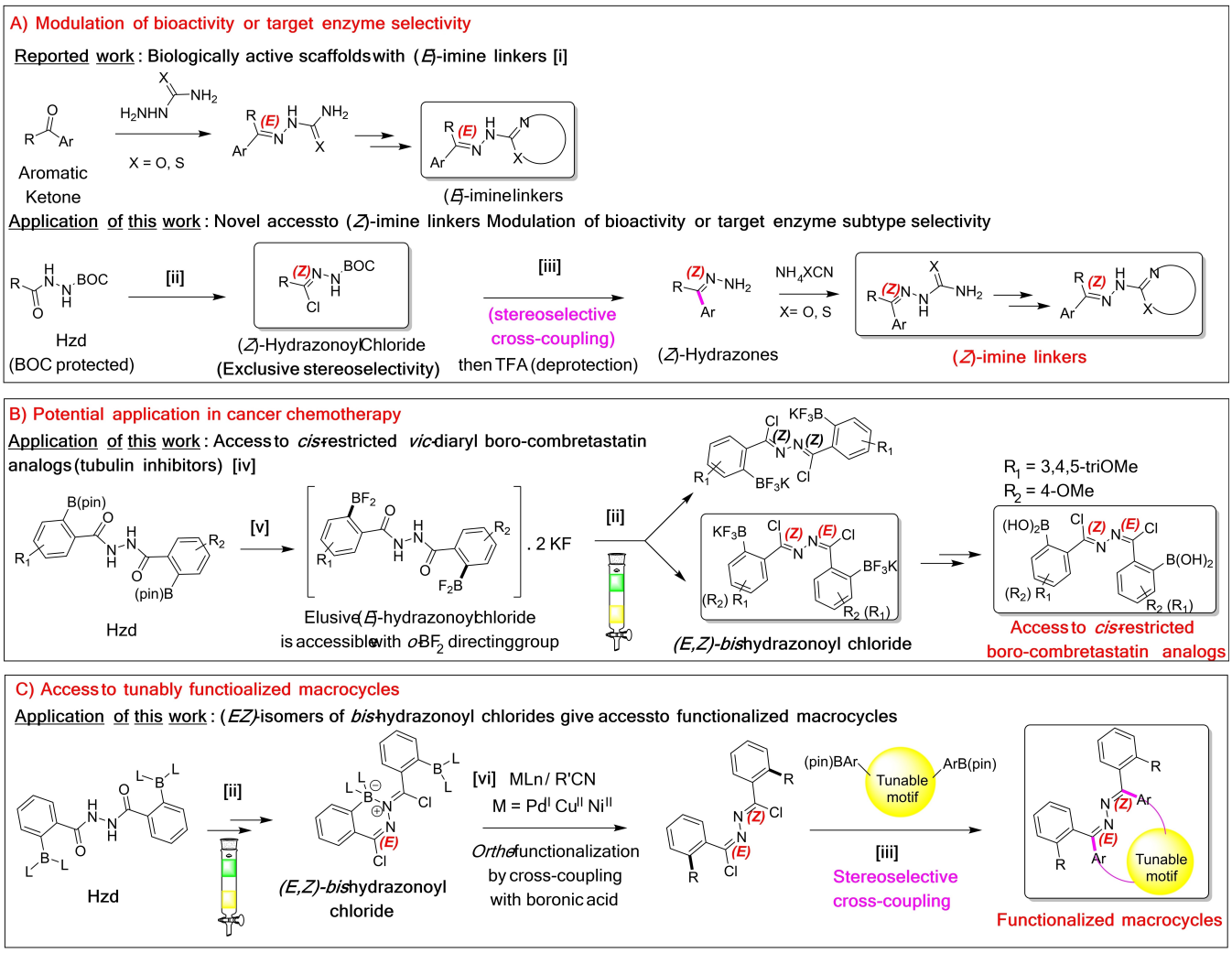

Figure 6. Promising applications in medicinal chemistry (**A** and **B**) and supramolecular chemistry (**C**) anticipated for the stereoselective synthesis of the chloroimidoyl (Cl–C=N) group by applying the synthetic and theoretical principles in this article. [i] Reported HCA II inhibitors as potential anticancer agents showing (*E*)-configuration of the C=N as proved by X-ray structural analysis;[75] [ii] PCl_5 (2.1 eq), C_6H_5Cl, 132 °C, 24 h (optimized procedure in this study); [iii] ArBpin, $Pd(PPh_3)_4$, Na_2CO_3 (2 M), DME, 80 °C, reported procedure;[83] [iv] reported borocombretastatin analogs as *cis*-restricted *vic*-diaryl tubulin inhibitors suitable for clinical trials;[81,82] [v] KHF_2(aq), MeOH/THF (1 : 1), 22 °C, 15 min, 92 %, reported procedure;[84] [vi] reported metal-catalyzed cross-coupling of organic nitriles and boronic acids.[85]

dized carbon,[83] while the functionalization would benefit from straightforward metal-catalyzed cross-coupling of organic nitriles and the *ortho*-boronic acid groups [116] (resulting from hydrolysis of the *o*-BF_2) (Figure 6c).

Furthermore, the field of protein modification has long been considered a hot topic, with wide scope applications in drug targeting, drug delivery, fluorescent labeling for cellular imaging … etc. It even gains much more interest when the reaction employed is bio-orthogonal (high-yielding, proceed rapidly and selectively in biological environments) and site-selective.[54] Among the common reactions employed is the click cycloaddition reaction of nitrilimines (in situ generated from a hydrazonoyl chloride precursor) to olefins (Figure 7A).

If a genetically modified protein bearing the proper olefinic moiety was treated with a properly substituted hydrazonoyl chloride derivative at physiologically compatible conditions, the resulting pyrazoline-modified protein would be easily obtained.[86–89] Although the hydrazonoyl chloride employed is not usually stereochemically characterized,[86] the swift generation of nitrilimine in the next step reflects a straightforward mechanism involving antiperiplanar chloride elimination which gives evidence of (Z)-geometry of the hydrazonoyl chloride precursor (as discussed earlier under the stereo-electronic factors affecting such elimination reactions).[32] Therefore, it should be a worthy application of this study to offer an exclusively stereoselective method of synthesizing the (*Z*)-hydrazonoyl chloride precursor required for further click protein modification (Figure 7A). Further ring-B substituent optimization (Figure 7A) could help reduce the possibility of the competing hydrolysis reaction of the nitrilimine.[88]

On the other side, the elusive (*E*)-isomer of hydrazonoyl chloride could find precious applications in site-specific protein modification (as well as the (*Z*)-isomer) but with a different mechanism. Unlike the (*Z*)-isomer, the (*E*)-isomer of the imidoyl

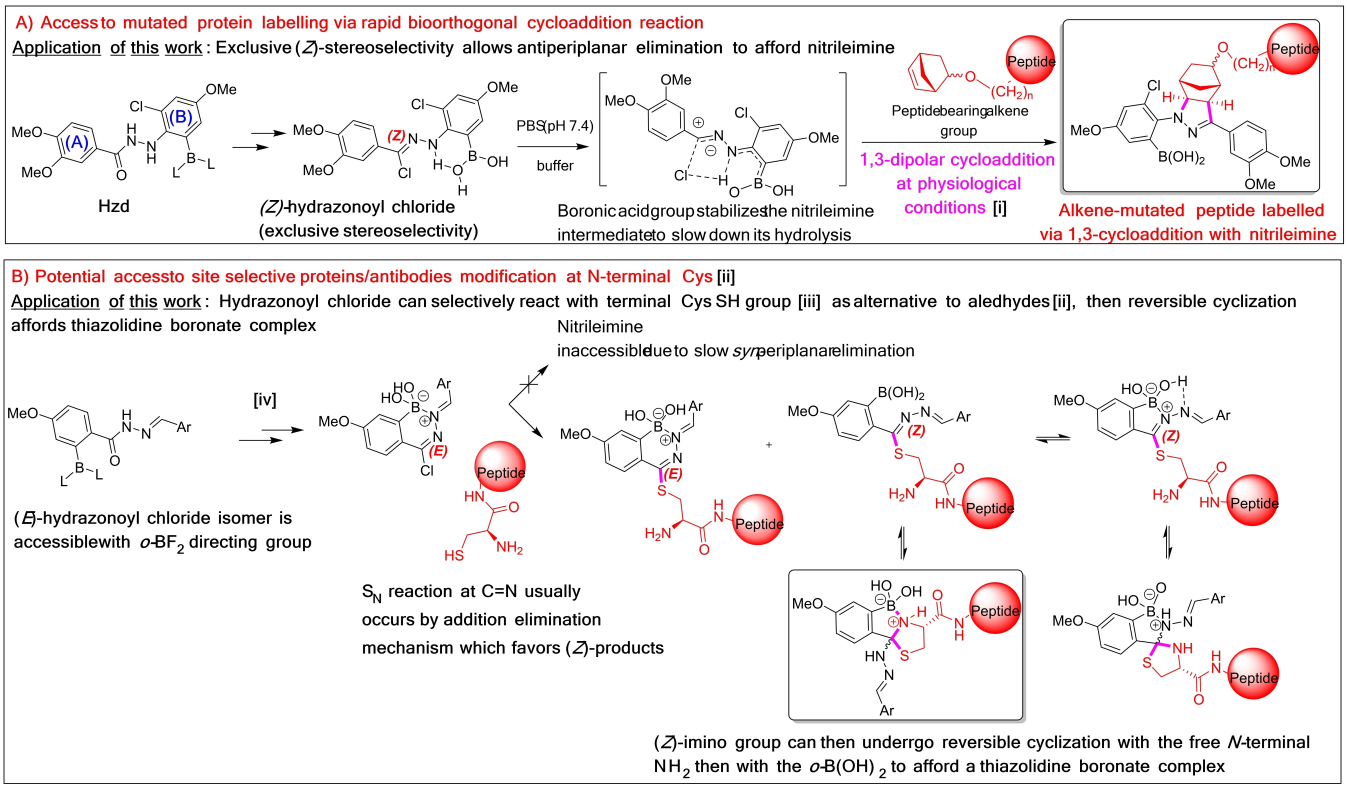

Figure 7. Promising applications in site-specific protein modification with both chloroimidoyl (Cl–C=N) group geometrical isomers. By applying the stereoselective synthetic principles in this article: **A**) the (*Z*)-isomer offers access to nitrilimines for click cycloaddition reaction with olefin modified proteins; and **B**) the (*E*)-isomer offers direct electrophilic motif for site-specific modification of N-terminal cysteine. [i] A well-established strategy for site selective protein labelling employing a click reaction of a genetically encoded olefinic C=C with nitrilimines prepared *in situ* via elimination of HCl from the precursor hydrazonoyl chloride at physiological conditions;[86–89] [ii] reported site-specific protein modification at N-terminal cysteine with aldehyde drugs affording a thiazolidine intermediate utilized for targeted delivery of cytotoxic agents;[90] [iii] reported S_N reaction of Cl–C=N group with cysteine SH at mild conditions[91] which recommends this group as an aldehyde alternative for site-specific protein modification; [iv] PCl_5 (2.1 eq), C_6H_5Cl, 132 °C, 24 h (optimized procedure in this study).

chloride (Cl–C=N–) functionality tends to be more resistant toward elimination reactions affording a nitrilimine due to stereo-electronic issues[32] (Figure 7B). Fortunately, this fact renders the (*E*)-isomer more amenable to direct nucleophilic substitution. Since the (*E*)-isomer of an open-chain imidoyl chloride (Cl–C=N–) functionality has never been purified and characterized (to our best knowledge), sufficient evidence of the reactivity of (*E*)-imidoyl chlorides could be gained by considering the 2-chloroazine heterocycles a representative subclass of (*E*)-imidoyl chlorides which are certainly reactive toward S_NAr mechanism.[92]

Accordingly, the closely related open-chain (*E*)-hydrazonoyl chloride scaffold could be employed for targeting cystine residues at N-terminals of proteins (Figure 7B). This provides an alternative to the reported aldehyde scaffold with a similar potential to afford a thiazolidine intermediate utilized for targeted delivery of cytotoxic agents.[90] Moreover, the recently reported S_N reaction of Cl–C=N group with cysteine SH at mild conditions[91] provides a proof of the concept. Furthermore, the key stereoselectivity modulator *o*-BF2 group could be further converted to the *o*-boronic acid which offers an access to a reversible thiadiazoline boronate complex with N-terminal Cys.[93]

Conclusions

Organic halogen compounds are cornerstones of applied chemical sciences. Halogen substitution is a smart molecular design strategy adopted to influence reactivity, membrane permeability and receptor interaction. The chiral environment of biological receptors usually imposes specific stereochemical requirements on the design and stereochemical optimization of successful ligands. Although there is remarkable advance in stereoselective halogenation methodology, the strategies are still catalyst-dependent and limited by the high expenses of the non-metal-based[94] or metal-based catalyst.[95,96] On the other side, PCl_5 is a classical halogenating agent which was reported to offer a solution to uncatalyzed stereoselective chlorination of alcohols via S_N2 and S_Ni mechanisms (with configurational inversion and retention, respectively) according to steric parameters. Unlike alcohols, the potential for chlorination of carbamoyl compounds (RCONHX, e.g. hydrazides, amides and hydroximates) have hardly been mechanistically studied from a stereochemical perspective to date.

Herein, we provide the first comprehensive stereochemical mechanistic explanation which outlines halogenation of *N,N'*-diacylhydrazines **Hzd** (as representative carbamoyl compounds)

with PCl_5, chemical optimization of hydrazonoyl chloride (**P2**) production, minimization of oxadiazole byproduct (**P1**), controlling the stereoselectivity output of **P2** to afford the desired (E)- or (Z)-stereoisomer of C(Cl)C=N group and providing summarized recommendations for potential applications of such stereoselectivity in drug design, protein modification and supramolecular chemistry (Figures 6 and 7).

The X-ray structural analysis unveiled an inherently exclusive stereoselectivity toward the production of (*Z*)-isomer of C(Cl)C=N group (**P2-ZZ**, Figure 2). Intriguingly, the few references which included similar halogenations of amides (**VIII**)[30,31] hydroximates (**V**)[32] and *N,N'*-diacylhydrazines (**XII**)[42] and proved the stereochemical outcomes have reported only the (*Z*)-products (Figure 1). On the other hand, the experimental optimization of the reaction conditions offered evidence that the desired *bis*-hydrazonoyl chloride (**P2**) can be regioselectively afforded only under thermodynamic conditions in non-polar solvents while introducing +M groups (regioselectivity parameter 1.82 and yield 63% for **P2-ZZ**$_{(4\text{-OMe})}$, Table 1).

Accordingly, DFT calculations of the overall reaction mechanism pathways have been covered while considering any reported intermediates potentially involved (e.g. pentacoordinate phosphoranol ethers[60,61]). The possibility of **Hzd** conformational isomerism[67–72] (Figure 4) and substituent effects (Figure 5) were also covered. Scheme 2 serves the most kinetically plausible mechanism highlighting three crucial discoveries.

Firstly, we discovered the key regioselectivity-limiting nitrilimine intermediate (**8-Z.HCl**) and why oxadiazole byproduct (**P1**) is more encountered under kinetic conditions (Tables S2–S6, Suppl. Mat.) in terms of **TS9** vs **TS10** competition for **8-Z.HCl**.

To validate such **P1**/**P2** product competition, we studied the kinetics of production of both spectrophotometrically and spectrofluorometrically (Suppl. Mat.), experimentally calculated the reaction order, the rate constants *k*1 and *k*2 (Equation 2), the difference between the free activation energies of the formation of **P1** and **P2-ZZ** ($\Delta\Delta G^{\ddagger}_{[P1/P2]}$) using Curtin-Hammett law (Equation 3) and finally compared this latter with the theoretically calculated one. To summarize, a small error (0.05 kcal/mol) of the calculated compared to the observed $\Delta\Delta G^{\ddagger}_{[P1/P2]}$ stands out as firm evidence of the validity of the suggested reaction mechanism (Scheme 2) and the reliability of the DFT calculation methodology (Suppl. Mat.).

The second discovery was the stereo-electronic factors influencing the exclusive production of (*Z*)-isomer of C(Cl)=N group (e.g. in **9-ZZ** and **P2-ZZ**), namely, the geometry of chloride addition to C–N multiple bond (**TS10** and **TS17-Z,anti**, respectively, Scheme 2). In both transition states, the newly emerging sp2 orbital carrying nitrogen lone pair and the attacking chloride nucleophile must be antiperiplanar. This result evokes that the reported nitrilimine intermediates (resembling **8-Z**) of a hydrazonoyl chloride origin (whether identified, isolated, *in-situ* generated or suggested) are all originating mainly from the (*Z*)-hydrazonoyl chloride isomer and successfully accounts for the X-ray evidenced exclusive production of (*Z*)-hydrazonoyl chlorides (e.g. **XIIa**[42] and **P2-ZZ**).

The third discovery was intriguing as it evoked two parallel stereoselectivity-influencing mechanisms representing stepwise and concerted elimination of HCl and $POCl_3$. As per the first halogenation (where there is neighboring OH participation in **2-ZZ**), the HCl elimination can proceed swiftly through unstrained nine-centre transition state (**TS5**) and subsequently the stepwise mechanism is more favored (**TS5** then **TS7-ZZ**). Concerning the second halogenation, the neighboring OH does not exist (**10-ZZ** and **10-ZE**) and hence concerted rate-limiting PCl4.Cl addition to C=O (**TS17** series) followed by rapid HCl elimination (**TS18** series) was found more kinetically favored than the angle-strained stepwise HCl elimination via **TS12-ZZ** and **TS12-ZE** (Figures S5, S11, and S13). To conclude, a better opportunity to obtain *E*-isomer of C(Cl)=N group is offered in the second halogenation step through **TS17-Z,syn** (vs **TS17-Z,anti**) which is mainly influenced by the relative stability of the Zwitterionic intermediates **10-ZZ** and **10-ZE** (Scheme 2, Figure 3).

Accordingly, we provide mechanism-inspired future recommendations for directing the halogenation reaction stereoselectivity toward elusive and stereochemically inaccessible (*E*)-carbamoyl halides (e.g. **P2-EZ**) by introducing *o*-BF_2 group as a neighboring substituent to enhance the stability of the precursor intermediate (here is **10-ZZ**) and provide access to the (E)-stereoselectivity rate-limiting transition state (here is **TS17-Z,syn**) and subsequently the (*E*)-carbamoyl halides in general (Scheme 3).

This approach of the uncatalyzed controlling of the (*E/Z*)-stereoselectivity of carbamoyl halide production along with introducing the synthetically tunable *o*-BF_2 group could find beneficial applications in biorthogonal reactions, medicinal chemistry, and protein modification (Figures 6 and 7). Finally, we believe the way to widely applied synthetic chemistry is paved by elaborate understanding of mechanisms of application-relevant reactions.

Experimental Section

Resource Availability

Lead Contact

Further information and requests for resources should be directed to and will be fulfilled by the lead contacts, Raed M. Maklad (raed.mostafa@pharm.kfs.edu.eg; rahm0072@uni.sydney.edu.au; raed mostafa2010@yahoo.com) and Gamal A. I. Moustafa (g.a.i.-moustafa@soton.ac.uk) upon request.

Supporting Information Summary and Data Availability Statement

All the synthesis methods, characterization charts and reports, crystallographic data and structural refinement for compound **P2-ZZ**, optimization of spectrometric assay of reaction products, optimization of reaction conditions, study of reaction kinetics, DFT calculation methods, energy scoring of all the optimized structures and their cartesian coordinates along with an extended discussion about the DFT study and the gained mechanistic conceptualiza-

tions are all outlined in the Supplementary Material (Suppl. Mat.) with relevant references along with short videos showing the imaginary frequencies vibrations of the key transition states in the proposed reaction mechanism. Further data requests will be responded to by the lead contact without restriction.

The X-ray structure of compound **P2-ZZ** was deposited on the Cambridge Crystallographic Data Centre (CCDC deposition number 2102606).

Additional references are cited within the Supporting Information.

Safety Statement

Caution! Phosphorus Pentachloride (CAS No. 10026–13-8) is fatal if inhaled [H330] and may cause damage to organs through prolonged or repeated exposure [H373]. Thionyl chloride (CAS No. 7719–09-7) is toxic if inhaled [H331] and may cause respiratory irritation [H335]. While both are harmful if swallowed [H302] and cause severe skin burns and eye damage [H314]. Hydrazine hydrate, 100% (CAS No. 10217–52-4) is GHS classified H226, H301 + H311 + H331, H314, H317, H350 and H410.

In this study, we controlled risk by using millimolar concentration of both, standard PPE, avoiding fume/dust inhalation and working under efficient fume hood.

Author Contributions

R. M. Maklad: Literature survey, design and implementation of synthesis and DFT studies, data analysis, mechanistic conceptualization, reaction kinetics study, results discussion and manuscript writing. G. A. I. Moustafa: Supervision, spectroscopic data analysis discussion of synthetic methodology and mechanistic principles, and manuscript revision. H. Aoyama: X-ray crystallographic analysis, structure solving and manuscript revision. A. A. Elgazar: spectrophotometric and spectrofluorometric analysis, results discussion and manuscript revision.

Acknowledgements

The authors pay deep thanks of gratitude to Asst Prof. Moataz A. Shaldam (Pharmaceutical Chemistry Dept, Faculty of Pharmacy, Kafrelsheikh University), Asst. Lect. Eman A. Elshenawy (Department of Pharmaceutical Analytical Chemistry, Faculty of Pharmacy, Tanta University) and Asst Prof. Galal Magdy (Pharmaceutical Analytical Chemistry Dept, Faculty of Pharmacy, Kafrelsheikh University) for their fruitful discussion about theoretical and experimental principles of fluorometric analysis. Deep thanks to Engr. Tarek M. Maklad (the High Institute of Engineering and Technology, New Minya, Egypt) for providing access to his computing facility. Sincere thanks to Asst. Prof. Morad M. El-Hendawy (Department of Chemistry, Faculty of Science, New Valley University, Kharga 72511, Egypt) for inspiring discussion about principles computational chemistry. The authors acknowledge Prof. Omar M. Aly and the Science and Technology Development Fund (STDF) (Project No. 2943 Basic and Applied Research, funded to Minia University, Egypt) for funding some of the chemicals and reagents utilized in this work. Finally, we thank Mr. Moamen AlBadry (Mathematics Education Consultant, Kingdom of Saudi Arabia) for helpful guidance with the mathematical equations of the kinetics study.

Conflict of Interests

The authors declare no competing interests.

Data Availability Statement

The data that support the findings of this study are available in the supplementary material of this article.

Keywords: DFT · Halogen · Hydrazonoyl halide · Protein modification · Reaction kinetics · Reaction mechanism · Stereoselectivity · X-ray structure

[1] V. Agarwal, Z. D. Miles, J. M. Winter, A. S. Eustáquio, A. A. El Gamal, B. S. Moore, *Chem. Rev.* **2017**, *117*, 5619–5674.
[2] M. H. Kolář, O. Tabarrini, *J. Med, Chem.* **2017**, *60*, 8681–8690.
[3] K. L. Brown, B. G. Hudson, P. A. Voziyan, *Curr. Opin. Nephrol. Hypertens.* **2018**, *27*, 171–175.
[4] G. Gerebtzoff, X. Li-Blatter, H. Fischer, A. Frentzel, A. Seelig, *ChemBioChem* **2004**, *5*, 676–684.
[5] M. Malakoutikhah, B. Guixer, P. Arranz-Gibert, M. Teixidó, E. Giralt, *ChemMedChem* **2014**, *9*, 1594–1601.
[6] C. L. Gentry, R. D. Egleton, T. Gillespie, T. J. Abbruscato, H. B. Bechowski, V. J. Hruby, T. P. Davis, *Peptides* **1999**, *20*, 1229–1238.
[7] R. M. Maklad, E.-S. M. N. AbdelHafez, D. Abdelhamid, O. M. Aly, *Bioorg. Chem.* **2020**, *99*, 103767.
[8] O. M. Aly, E. A. Beshr, R. M. Maklad, M. Mustafa, A. M. Gamal-Eldeen, *Arch. Pharm. (Weinheim)* **2014**, *347*, 658–667.
[9] D. Zhang, Y. Liu, C. Zhang, H. Zhang, B. Wang, J. Xu, L. Fu, D. Yin, C. Cooper, Z. Ma, Y. Lu, H. Huang, *Molecules* **2014**, *19*, 4380–4394.
[10] C. Lechner, M. Flaßhoff, H. Falke, L. Preu, N. Loaëc, L. Meijer, S. Knapp, A. Chaikuad, C. Kunick, *Molecules* **2019**, *24*, 4090.
[11] T. M. Ibrahim, G. Abada, M. Dammann, R. M. Maklad, W. M. Eldehna, R. Salem, M. M. Abdelaziz, R. A. El-domany, A. A. Bekhit, F. M. Beockler, *Eur. J. Med. Chem.* **2023**, *257*, 115534.
[12] Y. Shan, J. Lei, L. Zhang, T. Fan, M. Wang, Y. Ma, *Chem. Nat. Compd.* **2015**, *51*, 620–625.
[13] W. M. Eldehna, R. M. Maklad, H. Almahli, T. Al-Warhi, E. B. Elkaeed, M. A. S. Abourehab, H. A. Abdel-Aziz, A. M. El Kerdawy, *J. Enzyme Inhib. Med. Chem.* **2022**, *37*, 1227–1240.
[14] I. S. Marae, R. M. Maklad, S. Samir, E. A. Bakhite, W. Sharmoukh, *Drug Dev. Res.* **2023**, *84*, 747–766.
[15] M. J. Matos, S. Vilar, V. García-Morales, N. P. Tatonetti, E. Uriarte, L. Santana, D. Viña, *ChemMedChem* **2014**, *9*, 1488–1500.
[16] E. Mounetou, J. Legault, J. Lacroix, R. C. -Gaudreault, *J. Med. Chem.* **2003**, *46*, 5055–5063.
[17] R. B. Westkaemper, R. H. Abeles, *Biochemistry* **1983**, *22*, 3256–3264.
[18] Z. Wu, G. S. Minhas, D. Wen, H. Jiang, K. Chen, P. Zimniak, J. Zheng, *J. Med. Chem.* **2004**, *47*, 3282–3294.
[19] N. Mukerjee, M. Dryjanski, W. Dai, J. A. Katzenellenbogen, R. Pietruszko, *J. Protein Chem.* **1996**, *15*, 639–648.
[20] S. C. Wang, W. H. Johnson, R. M. Czerwinski, C. P. Whitman, *Biochemistry* **2004**, *43*, 748–758.
[21] G. A. Lyles, C. M. S. Marshall, I. A. McDonald, P. Bey, M. G. Palfreyman, *Biochem. Pharmacol.* **1987**, *36*, 2847–2853.
[22] K. M. Lee, W. J. Choi, Y. Lee, H. J. Lee, L. X. Zhao, H. W. Lee, J. G. Park, H. O. Kim, K. Y. Hwang, Y.-S. Heo, S. Choi, L. S. Jeong, *J. Med. Chem.* **2011**, *54*, 930–938.

[23] B. Gál, C. Bucher, N. Burns, *Mar. Drugs* **2016**, *14*, 206.
[24] D. A. Brumley, S. P. Gunasekera, Q.-Y. Chen, V. J. Paul, H. Luesch, *Org. Lett.* **2020**, *22*, 4235–4239.
[25] W. Chung, C. D. Vanderwal, *Angew. Chem. Int. Ed.* **2016**, *55*, 4396–4434.
[26] Q. Li, L. Zhou, X.-D. Shen, K.-C. Yang, X. Zhang, Q.-S. Dai, H.-J. Leng, Q.-Z. Li, J.-L. Li, *Angew. Chem. Int. Ed.* **2018**, *57*, 1913–1917.
[27] C. Wang, H. Yamamoto, *Org. Lett.* **2014**, *16*, 5937–5939.
[28] C. W. Shoppee, J. C. Coll, *J. Chem. Soc. C* **1970**, 1124–1125■■Please provide missing volume number for the reference [28]■■.
[29] R. Carman, I. Shaw, *Aust. J. Chem.* **1976**, *29*, 133.
[30] A. Lévesque, T. Maris, J. D. Wuest, *J. Am, Chem. Soc.* **2020**, *142*, 11873–11883.
[31] D. Lindauer, R. Beckert, M. Döring, P. Fehling, H. Görls, *J. Für Prakt. ChemieChemiker-Ztg.* **1995**, *337*, 143–152.
[32] J. E. Johnson, E. C. Riesgo, I. Jano, *J. Org. Chem.* **1996**, *61*, 45–50.
[33] M. Bortoluzzi, F. Marchetti, M. G. Murrali, G. Pampaloni, *Inorganica Chim. Acta* **2015**, *427*, 150–154.
[34] G. Bresciani, F. Marchetti, G. Pampaloni, *Coord. Chem. Rev.* **2023**, *496*, 215399.
[35] C. W. Shoppee, M. E. H. Howden, R. Lack, *J. Chem. Soc.* **1960**, 4874–4879■■Please provide missing volume number for the reference [35]■■.
[36] V. V. Il'in, O. V. Slavinskaya, Yu. A. Strelenko, A. V. Ignatenko, V. A. Ponomarenko, *Bull. Acad. Sci. USSR Div. Chem. Sci.* **1991**, *40*, 2177–2180.
[37] Z. Guo, H. Jia, H. Liu, Q. Wang, J. Huang, H. Guo, *Org. Lett.* **2018**, *20*, 2939–2943.
[38] H. A. Abdel-Aziz, A. A. I. Mekawey, *Eur. J. Med. Chem.* **2009**, *44*, 4985–4997.
[39] W. Long, S. Chen, X. Zhang, L. Fang, Z. Wang, *Tetrahedron* **2018**, *74*, 6155–6165.
[40] R. E. Khidre, H. A. Mohamed, B. M. Kariuki, G. A. El-Hiti, *Phosphorus Sulfur Silicon Relat. Elem.* **2020**, *195*, 29–36.
[41] Y.-Z. Jiang, *Chin. J. Synth. Chem.* **2006**, *14*, 355–359.
[42] V. K. Tandon, A. Sharon, R. Bandichhor, P. R. Maulik, *Acta Crystallogr. Sect. E Struct. Rep. Online* **2002**, *58*, o869–o870.
[43] A. Schnell, J. A. Willms, S. Nozinovic, M. Engeser, *Beilstein J. Org, Chem.* **2019**, *15*, 30–43.
[44] Z. Zhou, Y. Zhang, S. Liu, Z. Chi, X. Chen, J. Xu, *J. Mater. Chem. C* **2016**, *4*, 10509–10517.
[45] V. M. Tsefrikas, S. Arns, P. M. Merner, C. C. Warford, B. L. Merner, L. T. Scott, G. J. Bodwell, *Org. Lett.* **2006**, *8*, 5195–5198.
[46] K.-P. Hartmann, M. Heuschmann, *Tetrahedron* **2000**, *56*, 4213–4218.
[47] A. S. Shawali, M. A. N. Mosselhi, *J. Heterocycl. Chem.* **2003**, *40*, 725–746.
[48] S. K. Liew, A. Holownia, A. J. Tilley, E. I. Carrera, D. S. Seferos, A. K. Yudin, *J. Org, Chem.* **2016**, *81*, 10444–10453.
[49] V. V. Voronin, M. S. Ledovskaya, E. G. Gordeev, K. S. Rodygin, V. P. Ananikov, *J. Org. Chem.* **2018**, *83*, 3819–3828.
[50] T. Al-Warhi, H. Almahli, R. M. Maklad, Z. M. Elsayed, M. A. El Hassab, O. J. Alotaibi, N. Aljaeed, R. R. Ayyad, H. A. Ghabour, W. M. Eldehna, M. K. El-Ashrey, *Molecules* **2023**, *28*, 3203.
[51] A. S. Shawali, *Curr. Org. Chem.* **2010**, *14*, 784–815.
[52] A. S. Shawali, *J. Adv, Res.* **2016**, *7*, 873–907.
[53] A. S. Shawali, N. A. Samy, *Open Bioact. Compd. J.* **2009**, *2*, 8–16.
[54] O. Boutureira, G. J. L. Bernardes, *Chem. Rev.* **2015**, *115*, 2174–2195.
[55] H. Khalilullah, M. J. Ahsan, M. Hedaitullah, S. Khan, B. Ahmed, *Mini-Rev. Med. Chem.* **2012**, *12*, 789–801.
[56] X. Li, H. Ye, D. Chen, K. Liu, G. Xie, Y. Wang, C. Lo, A. Lien, J. Peng, Y. Cao, S. Su, *Isr. J. Chem.* **2014**, *54*, 971–978.
[57] M. M. Al-Sanea, G. H. Al-Ansary, Z. M. Elsayed, R. M. Maklad, E. B. Elkaeed, M. A. Abdelgawad, S. N. A. Bukhari, M. M. Abdel-Aziz, H. Suliman, W. M. Eldehna, *J. Enzyme Inhib. Med. Chem.* **2021**, *36*, 987–999.
[58] T. Al-Warhi, D. M. Elimam, Z. M. Elsayed, M. M. Abdel-Aziz, R. M. Maklad, A. A. Al-Karmalawy, K. Afarinkia, M. A. S. Abourehab, H. A. Abdel-Aziz, W. M. Eldehna, *RSC Adv.* **2022**, *12*, 31466–31477.
[59] R. M. Maklad, *M.Sc. Thesis*, Minia University (EG) **2017**, DOI: 10.13140/RG.2.2.18711.29601 (accessed: 30 June 2024)■■Please check edit made in reference [59]■■.
[60] K. Han, Y. Wang, P. Zhao, X. You, J. Wang, Y. Guo, Y. Zhao, S. Cao, *J. Org. Chem.* **2021**, *86*, 4512–4531.
[61] L. D. Quin, J. G. Verkade, Eds, *Phosphorus Chemistry: Proceedings of the 1981 International Conference*, American Chemical Society, Washington, D. C. **1981**■■Please provide complete details for the reference [61]■■.
[62] M. Giustiniano, V. Mercalli, J. Amato, E. Novellino, G. C. Tron, *Org. Lett.* **2015**, *17*, 3964–3967.
[63] G. Fodor, S. Nagubandi, *Tetrahedron* **1980**, *36*, 1279–1300.
[64] P. Deslongchamps, *Stereoelectronic Effects in Organic Chemistry*, Pergamon Pr, Oxford **1989**.
[65] X. Li, M. J. Frisch, *J. Chem, Theory Comput.* **2006**, *2*, 835–839.
[66] M. Smith, J. March, *March's Advanced Organic Chemistry: Reactions, Mechanisms, and Structure*, Wiley-Interscience, Hoboken, N. J. **2007**.
[67] B. Price, I. O. Sutherland, F. G. Williamson, *Tetrahedron* **1966**, *22*, 3477–3490.
[68] I. D. Kalikhman, O. B. Bannikova, E. N. Medvedeva, T. I. Yushmanova, V. A. Lopyrev, *Bull. Acad. Sci. USSR Div. Chem. Sci.* **1982**, *31*, 1275–1277.
[69] O. Tšubrik, P. Burk, T. Pehk, U. Mäeorg, *J. Mol. Struct. THEOCHEM* **2001**, *546*, 119–125.
[70] J. K. R. Deka, B. Sahariah, S. S. Sakpal, A. K. Bar, S. Bagchi, B. K. Sarma, *Org. Lett.* **2021**, *23*, 7003–7007.
[71] J. K. R. Deka, B. Sahariah, K. Baruah, A. K. Bar, B. K. Sarma, *Chem. Commun.* **2020**, *56*, 4874–4877.
[72] I. D. Kalikhman, P. V. Makerov, E. N. Medvedeva, T. I. Yushmanova, V. A. Lopyrev, *Bull. Acad. Sci. USSR Div. Chem. Sci.* **1979**, *28*, 1760–1764.
[73] J. I. Seeman, *J. Chem, Educ.* **1986**, *63*, 42.
[74] J. I. Seeman, *Chem. Rev.* **1983**, *83*, 83–134.
[75] A. Kumar, K. Siwach, T. Rom, R. Kumar, A. Angeli, A. Kumar Paul, C. T. Supuran, P. K. Sharma, *Bioorg. Chem.* **2022**, *123*, 105764.
[76] S. Gomha, S. Ahmed, A. Abdelhamid, *Molecules* **2015**, *20*, 1357–1376.
[77] P. A. Elzahhar, S. M. Abd El Wahab, M. Elagawany, H. Daabees, A. S. F. Belal, A. F. EL-Yazbi, A. H. Eid, R. Alaaeddine, R. R. Hegazy, R. M. Allam, M. W. Helmy, B. Elgendy, A. Angeli, S. A. El-Hawash, C. T. Supuran, *Eur. J. Med. Chem.* **2020**, *200*, 112439.
[78] T. A. Bakka, M. B. Strøm, J. H. Andersen, O. R. Gautun, *Bioorg. Med. Chem.* **2017**, *25*, 5380–5395.
[79] N.-H. Nam, *Curr. Med. Chem.* **2003**, *10*, 1697–1722.
[80] J. Kaffy, R. Pontikis, J.-C. Florent, C. Monneret, *Org. Biomol. Chem.* **2005**, *3*, 2657.
[81] Y. Kong, J. Grembecka, M. C. Edler, E. Hamel, S. L. Mooberry, M. Sabat, J. Rieger, M. L. Brown, *Chem. Biol.* **2005**, *12*, 1007–1014.
[82] H. Nakamura, H. Kuroda, H. Saito, R. Suzuki, T. Yamori, K. Maruyama, T. Haga, *ChemMedChem* **2006**, *1*, 729–740.
[83] A. Casimiro-Garcia, D. W. Piotrowski, C. Ambler, G. B. Arhancet, M. E. Banker, T. Banks, C. M. Boustany-Kari, C. Cai, X. Chen, R. Eudy, D. Hepworth, C. A. Hulford, S. M. Jennings, P. M. Loria, M. J. Meyers, D. N. Petersen, N. K. Raheja, M. Sammons, L. She, K. Song, D. Vrieze, L. Wei, *J. Med. Chem.* **2014**, *57*, 4273–4288.
[84] J. Roose, A. C. S. Leung, J. Wang, Q. Peng, H. H.-Y. Sung, I. D. Williams, B. Z. Tang, *Chem. Sci.* **2016**, *7*, 6106–6114.
[85] H. N. Dhara, A. Rakshit, T. Alam, B. K. Patel, *Org. Biomol. Chem.* **2022**, *20*, 4243–4277.
[86] Y. Kurra, K. A. Odoi, Y.-J. Lee, Y. Yang, T. Lu, S. E. Wheeler, J. Torres-Kolbus, A. Deiters, W. R. Liu, *Bioconjug. Chem.* **2014**, *25*, 1730–1738.
[87] E. Kaya, M. Vrabel, C. Deiml, S. Prill, V. S. Fluxa, T. Carell, *Angew. Chem. Int. Ed.* **2012**, *51*, 4466–4469.
[88] Y.-J. Lee, B. Wu, J. E. Raymond, Y. Zeng, X. Fang, K. L. Wooley, W. R. Liu, *ACS Chem. Biol.* **2013**, *8*, 1664–1670.
[89] X. S. Wang, Y.-J. Lee, W. R. Liu, *Chem. Commun.* **2014**, *50*, 3176–3179.
[90] G. Casi, N. Huguenin-Dezot, K. Zuberbühler, J. Scheuermann, D. Neri, *J. Am. Chem. Soc.* **2012**, *134*, 5887–5892.
[91] S. R. Kasibhatla, S. Sharma, M. Kaadige, A. Weston, S. Dana, T. Thode, The Translational Genomics Research Institute. Imidazopyridazine and Imidazopyrazine Compounds as Inhibitors of CDK7. WO2022061155 A1 **2022**■■Please provide complete details for the reference [91]■■.
[92] T. Chan, J. Miller, *Aust. J. Chem.* **1967**, *20*, 1595.
[93] Y. Tan, J. Wu, L. Song, M. Zhang, C. J. Hipolito, C. Wu, S. Wang, Y. Zhang, Y. Yin, *Int. J. Mol. Sci.* **2021**, *22*, 12958.
[94] S. Liu, B. Zhang, W. Xiao, Y. Li, J. Deng, *Adv. Synth. Catal.* **2022**, *364*, 3974–4005.
[95] D. A. Petrone, J. Ye, M. Lautens, *Chem. Rev.* **2016**, *116*, 8003–8104.
[96] M. Bortoluzzi, G. Bresciani, F. Marchetti, G. Pampaloni, S. Zacchini, *Dalton Trans.* **2015**, *44*, 10030–10037.

Manuscript received: February 27, 2024
Accepted manuscript online: July 3, 2024
Version of record online: ■■, ■■

RESEARCH ARTICLE

Due to the increasing interest in halo compounds in chemotherapy and protein modification/targeting in chiral bioenvironments, controlling the halogenation stereoselectivity is state-of-the-art science. Halogenation of carbamoyl group (–NHC=O) has never been mechanistically studied. Herein, we dive into depths of regioselectivity and stereoselectivity, provide the first comprehensive mechanism highlighting the selectivity-limiting factors and provide subsequent inspirations to control the (*E/Z*)-stereochemical output and insights into multidisciplinary applications.

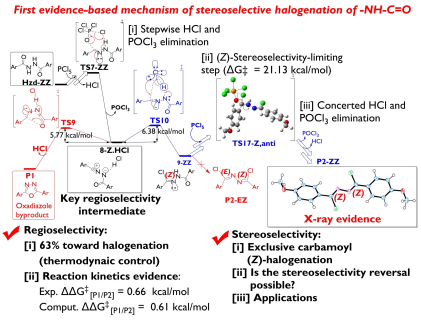

R. M. Maklad, G. A. I. Moustafa*, H. Aoyama, A. A. Elgazar*

1 – 21

Controlling (E/Z)-Stereoselectivity of –NHC=O Chlorination: Mechanism Principles for Wide Scope Applications

@Raed_M_Maklad @SpecElgazar

Share your work on social media! *Chemistry - A European Journal* has added Twitter as a means to promote your article. Twitter is an online microblogging service that enables its users to send and read short messages and media, known as tweets. Please check the pre-written tweet in the galley proofs for accuracy. If you, your team, or institution have a Twitter account, please include its handle @username. Please use hashtags only for the most important keywords, such as #catalysis, #nanoparticles, or #proteindesign. The ToC picture and a link to your article will be added automatically, so the **tweet text must not exceed 250 characters**. This tweet will be posted on the journal's Twitter account (follow us @ChemEurJ) upon publication of your article in its final form. We recommend you to re-tweet it to alert more researchers about your publication, or to point it out to your institution's social media team.

ORCID (Open Researcher and Contributor ID)

Please check that the ORCID identifiers listed below are correct. We encourage all authors to provide an ORCID identifier for each coauthor. ORCID is a registry that provides researchers with a unique digital identifier. Some funding agencies recommend or even require the inclusion of ORCID IDs in all published articles, and authors should consult their funding agency guidelines for details. Registration is easy and free; for further information, see http://orcid.org/.

Hiroshi Aoyama http://orcid.org/0000-0001-7915-8975
Raed M. Maklad http://orcid.org/0000-0002-5219-4842
Gamal A. I. Moustafa http://orcid.org/0000-0002-9940-0033
Abdullah A. Elgazar http://orcid.org/0000-0002-5851-3306

Author Contributions

Raed M. Maklad: Conceptualization:Lead; Data curation:Lead; Formal analysis:Lead; Funding acquisition:Equal; Investigation:Lead; Methodology:Lead; Project administration:Lead; Resources:Lead; Software:Lead; Validation: Lead; Visualization:Lead; Writing – original draft:Lead; Writing – review & editing:Lead
Gamal A. I. Moustafa: Conceptualization:Supporting; Data curation:Supporting; Project administration:Supporting; Resources:Supporting; Supervision:Lead; Writing – review & editing:Lead
Hiroshi Aoyama: Data curation:Supporting; Formal analysis:Lead; Methodology:Supporting; Resources:Supporting; Writing – original draft:Supporting; Writing – review & editing:Supporting
Abdullah A. Elgazar: Formal analysis:Lead; Funding acquisition:Equal; Methodology:Supporting; Resources: Supporting; Writing – review & editing:Supporting